NUMERICAL EXPERIMENTS PERTAINING TO WARM-FOG SUPPRESSION

L. R. Koenig

Rand Corporation
Santa Monica, California

October 1969

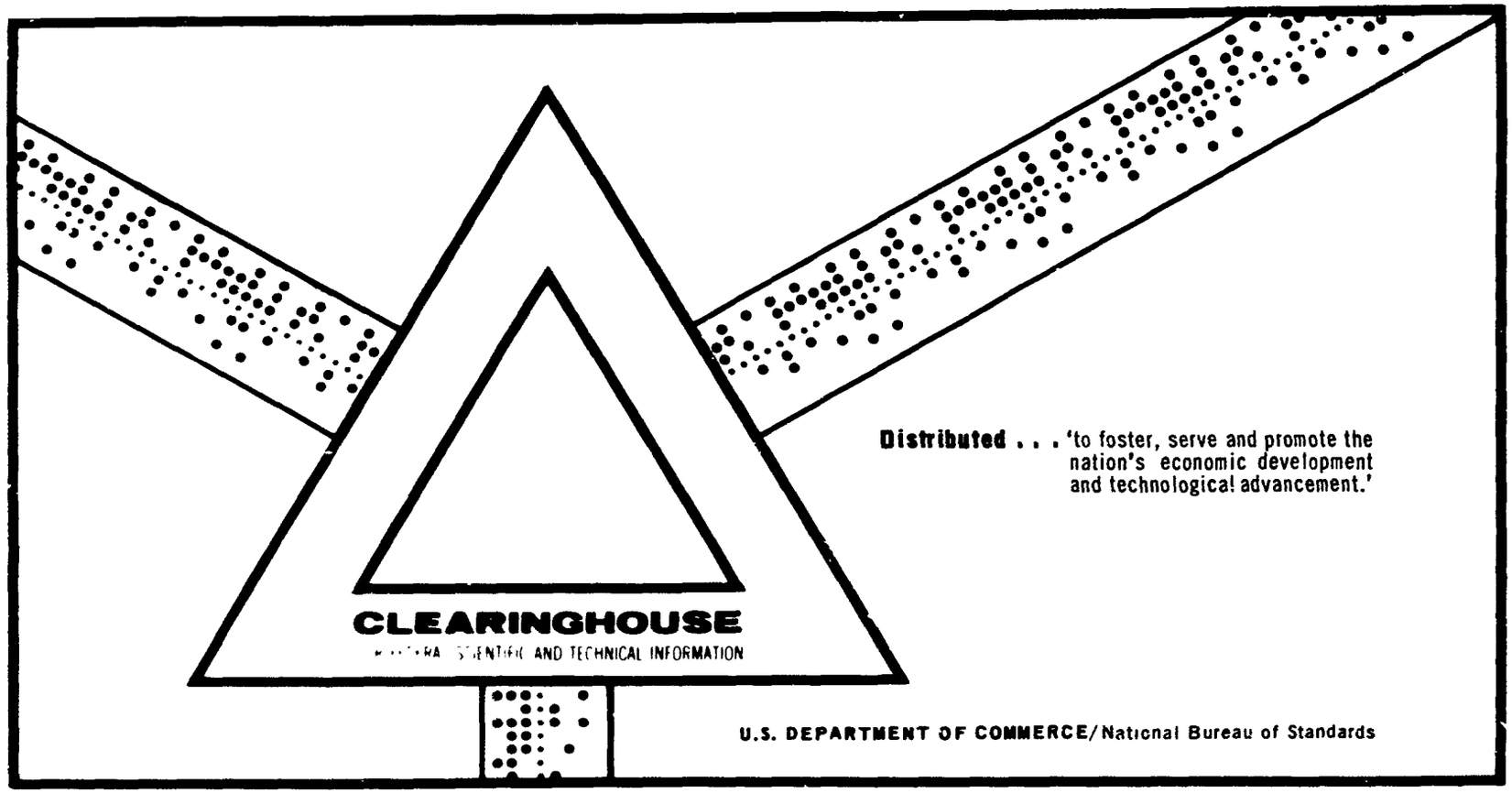

MEMORANDUM
RM-6159-PR
OCTOBER 1969

NUMERICAL EXPERIMENTS PERTAINING TO WARM-FOG SUPPRESSION

L. R. Koenig

PREPARED FOR:

UNITED STATES AIR FORCE PROJECT RAND

The RAND Corporation
SANTA MONICA • CALIFORNIA

57

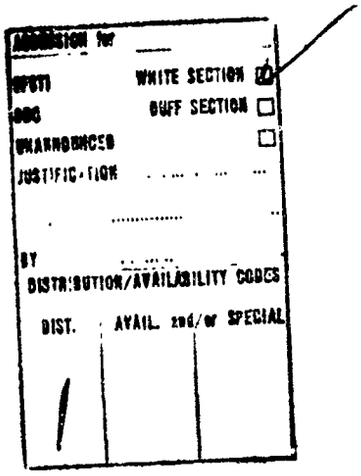
WHITE SECTION
BUFF SECTION
DISTRIBUTION/AVAILABILITY CODES
DIST.
AVAIL. and/or SPECIAL

MEMORANDUM
RM-6159-PR
OCTOBER 1969

NUMERICAL EXPERIMENTS PERTAINING TO WARM-FOG SUPPRESSION

L. R. Koenig

This research is supported by the United States Air Force under Project RAND—Contract No. F44620-67-C-0045 monitored by the Directorate of Operational Requirements and Development Plans, Deputy Chief of Staff, Research and Development, Hq USAF. Views or conclusions contained in this study should not be interpreted as representing the official opinion or policy of the United States Air Force.

The RAND Corporation

This study is presented as a competent treatment of the subject, worthy of publication. The Rand Corporation vouches for the quality of the research, without necessarily endorsing the opinions and conclusions of the authors.

Published by The RAND Corporation

PREFACE

This Memorandum reports on one aspect of RAND's continuing investigation of weather and climate. The aim of these studies is to contribute both to the understanding of processes controlling weather and climate and to the investigation of methods by which these natural processes might be changed -- either by design or inadvertently. Closely related work on the micro and macro scale by RAND staff members includes work on the mathematical simulation of cloud dynamics by F. W. Murray, investigation of the hydrodynamics and statistics of droplet interaction and coalescence by M. H. Davis, M. Warshaw, and C. L. Olson, and studies of micro-physical diffusion processes and cloud glaciation by L. R. Koenig.

The mathematical simulation of the growth of cloud droplets by condensation is described in detail in RM-5553-NSF. That work formed the basis for the present investigation into prospects for warm-fog modification by means of condensation-nucleus seeding.

ABSTRACT

As part of a continuing study of micro-physical aspects of weather processes, an attempt has been made quantitatively to assess the prospects for modifying warm fogs by seeding them with condensation nuclei. This has been done by calculating the time-dependent changes in the sizes and concentrations of fog droplets that are predicted by the ordinary equations of diffusion of water vapor to and from the surface of droplets, taking into account their size, molality, and ambient water-vapor density.

Initial conditions consist of a homogeneous volume of air of specified height and aerosol content. An external cooling rate and seed dosage are specified. The effects of various combinations of cloud height, seed properties (such as size, mass density, and rate of injection) on the metamorphosis of the fog-droplet population are examined. The cloud-forming process (in which temperature decreases with time) is allowed to continue after seeding has been accomplished, and tentative conclusions are drawn regarding the ranges of seed dosages that might result in successful and nonsuccessful efforts to suppress warm fog.

A discussion of the basis of calculations of the meteorological range is included.

SYMBOLS

B	brightness, candle cm^{-2}
C	brightness contrast
D	mass diffusion coefficient of water vapor in air, 0.226 $cm^2 sec^{-1}$
d	depth of fog layer, cm
e	water vapor pressure, dyne cm^{-2}
I	intensity, candle
i	van't Hoff factor
J	mechanical equivalent of heat, 5.8×10^{-5} cal cm^{-1} $°K^{-1} sec^{-1}$
K_s	scattering-area coefficient
L	latent heat of condensation, 594.4 cal g^{-1}
M	molecular mass, g mol^{-1}
m	mass, grams
n	concentration, cm^{-3}
R	universal gas constant, 8.314×10^7 erg mol^{-1} $°K^{-1}$
r	radius, cm
S	supersaturation
T	absolute temperature, °K
t	time, sec
V	terminal velocity, cm sec^{-1}
x	path length, cm^{-1}
σ	extinction coefficient, cm^{-1}
τ	surface tension, 75.7 dyne cm^{-1}
Ψ	spectral sensitivity of human eye

Subscripts

a	air
j	drop-size index
n	nucleus
r	on x, meteorological range
s	saturated, sky or background
sfc	at surface of drop
T_{sfc}	at drop surface temperature
T_{∞}	at ambient temperature
v	virtual (see text)
w	water
λ	specific frequency of light
*	corrected value of e or e_s considering size and molality of drop
∞	ambient

CONTENTS

PREFACE iii

ABSTRACT v

SYMBOLS vii

Section
I. INTRODUCTION 1

II. PRINCIPLE INVOLVED IN WARM-FOG MODIFICATION BY SALT SEEDING 2

III. BASIS OF CALCULATIONS 12
Calculation of Transparency of Fog 12
Calculation of Droplet Evolution 20
The Fog Model 21

IV. RESULTS 23
Verification of the Numerical Model 23
Effect of Seed Quantity 31
Effect of Seed Size 35
Effect of Differences in Fog Thickness 39
Effects of Variations in Rapidity of Dispersal 41
Effect of Differences in Natural Aerosol Concentration and Size Distribution 42
Effect of Monodispersed Seed Particles in Contrast to that of Polydispersed Seed Particles 44
Effect of Droplet Fallout 46

V. CONCLUSIONS 47

REFERENCES 49

I. INTRODUCTION

The improvement of visibility in a fog has been one of the persistent goals of weather modification. This might be accomplished either by reducing the water content of fog or by shifting the size distribution of fog droplets toward larger droplets. The first might be achieved by warming the fog mass; the second forms the basis of modifying supercooled fog by seeding with ice-forming nuclei. In this Memorandum we are concerned with the problem of applying seeding techniques to natural "warm" fogs; i.e., fogs composed of droplets warmer than 0°C.

Warm fogs are in equilibrium with respect to phase transition, and unlike supercooled fogs, are not amenable to artificial modification by exploitation of a latent phase instability. It has long been recognized that in principle, one may improve visibility by seeding warm fogs with large condensation nuclei that redistribute the water content from the many small atmospheric nuclei onto the few large artificial nuclei. Technical problems related to the manufacture and dispersal of the seed particles have hampered the development of warm-fog seeding technology, but these appear to be on the threshold of solution. Anticipating the technical feasibility of condensation-nucleus seeding, we attempt in this Memorandum, on the basis of numerical simulation techniques, to examine warm-fog seeding prospects and to identify factors critical to the success or failure of such ventures.

II. PRINCIPLE INVOLVED IN WARM-FOG MODIFICATION BY SALT SEEDING

A natural fog forms when a parcel of air cools below its dew point. (At relative humidities greater than about 70 percent but less than 100 percent, a distinct haze forms -- reducing visibility, but not enough to hinder ordinary activities). The fog droplets form on aerosol particles, which are always present in the atmosphere. Generally the number density of aerosol particles is much higher in terrestrial air masses than in oceanic air masses, but even in a given air mass, the concentration of aerosols is markedly variable. In general, the relative concentration reaches a peak near a particle size having a Stokes diameter* of about 0.3μ, regardless of either the absolute concentration or the origin of the air mass. Data on the concentration of droplets as a function of supersaturation (Wieland, 1956) suggest that the peak in relative concentration should be at a diameter of about 0.18μ if it is assumed that natural aerosol particles are composed of NaCl, as we do in this work.

Each aerosol particle is a latent center of condensation, and is consequently a potential fog droplet. By the same token, each particle is a potential cause of reduced visibility. In fact, however, not every particle will become a fog droplet, even if the air becomes cooled below its dew point. Whether an aerosol particle becomes a fog droplet or remains a haze particle depends upon whether the droplet embryo is exposed to supersaturation greater than a critical value over a time sufficiently long for the droplet to grow beyond a critical size. The critical size and the supersaturation are both a function of the mass and the chemical composition of the nucleus. These critical values arise from the fact that the vapor pressure over a curved surface is an inverse function of the radius of curvature and the molality of a drop. For a given nucleus, the smaller the drop, the greater are both the curvature and the solution effects, one acting to lower the vapor pressure and the other to raise it with

---

*The diameter of a sphere of unit density, which under the influence of gravity has the same terminal velocity as the unknown particle.

respect to the vapor pressure over a pure, plane surface. As a result of these opposing influences, maximum equilibrium vapor pressures over droplets occur at specific sizes that are functions of the amount and kind of soluble matter in the droplet. These are the critical sizes and critical vapor pressures for specific nuclei. The Kelvin and Raoult equations, which relate molality, drop size, and vapor pressure, may be combined and simplified to yield approximate equations for the critical values (see, for example, Fletcher, 1962), viz.:

$$r_c = \left(\frac{3.91 \times 10^5 \; i m_n T}{M_n} \right)^{1/2} \quad \text{(cm)} \tag{2.1}$$

$$s_c = \left(\frac{1.238 \times 10^{-11} \; M_n}{i m_n T^3} \right)^{1/2} \quad \text{(percent)} \tag{2.2}$$

Figure 1 shows curves of equilibrium vapor pressure over a drop as a functior of size and nucleus content. These "Köhler" curves show results of the size and solution effects and critical values of size and supersaturation. Figure 2 shows the critical radius and critical supersaturation as a function of nucleus size for salt (NaCl) at 0°C.

The importance of the critical saturation may be appreciated when one realizes that only nuclei having sizes equal to or larger than the critical value corresponding to the maximum supersaturation achieved during the fog-formation process will grow into fog droplets; the remainder, restricted to sizes below their critical value, will not materially reduce the distance at which an object can be recognized, and are not normally regarded as fog particles. Thus with a given size distribution of nuclei, the number of nuclei activated, and hence the fog-droplet concentration and the restrictions on visibility, will be a function of the maximum supersaturation experienced during the formation of the fog. (The supersaturation itself

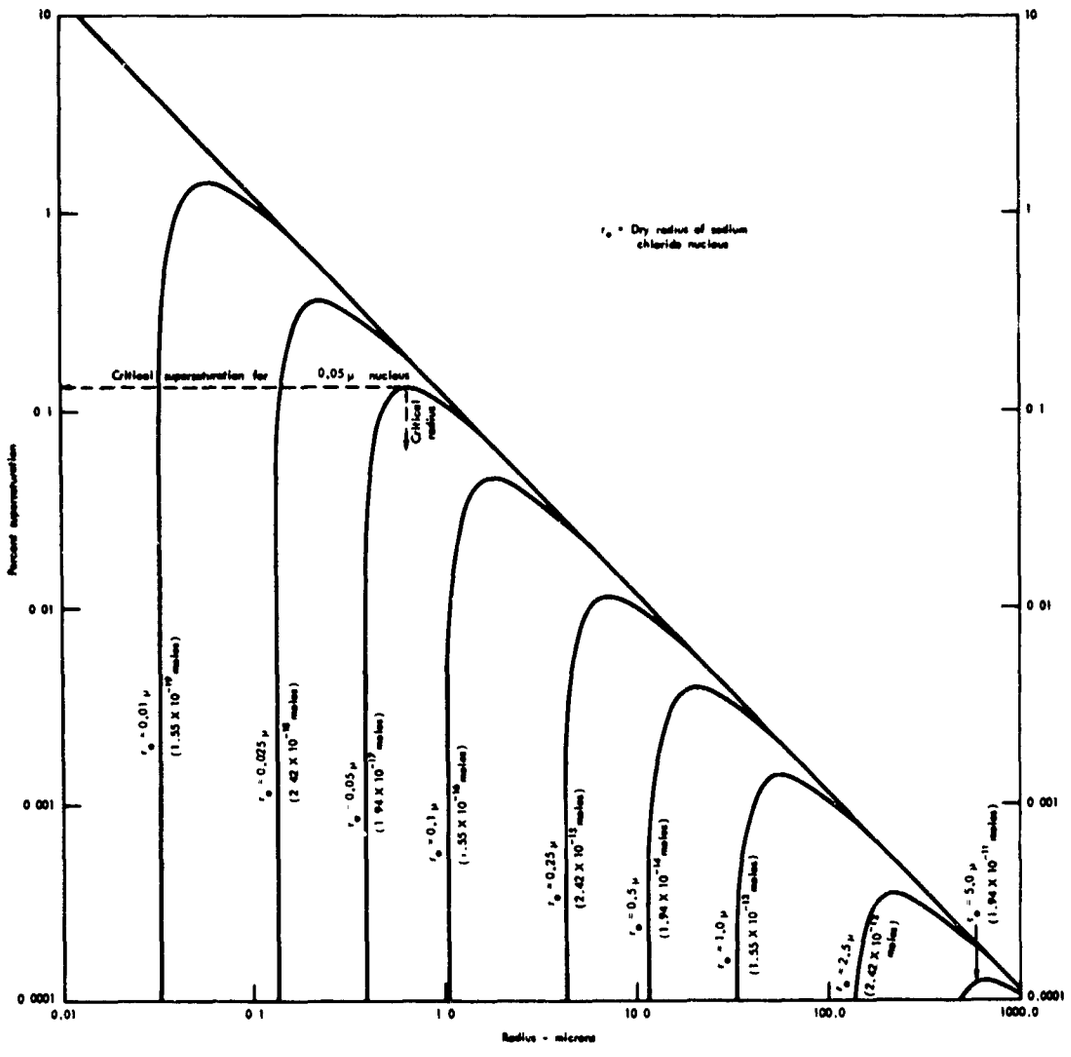

Fig. 1 -- Equilibrium vapor density relative to that of plane, pure water for water droplets containing various quantities of sodium chloride particles (Köhler curves).

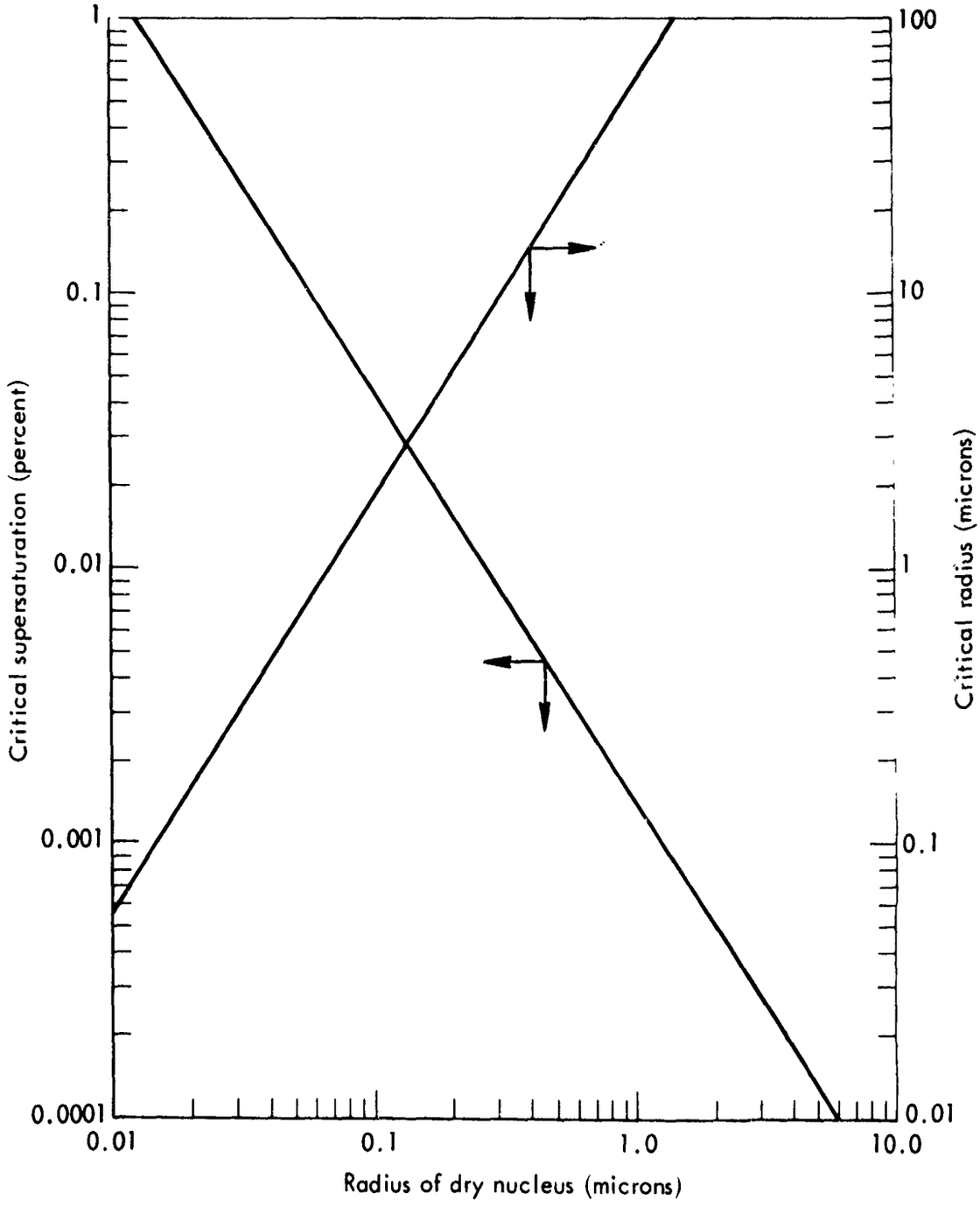

Fig. 2 -- Critical radius of droplet and corresponding critical ambient supersaturation for droplets containing various quantities of sodium chloride.

is a function of the meteorological process responsible for formation of the fog and of the nucleus content of the air.) The fog-suppression schemes investigated in this Memorandum involve either the removal of water content from the fog by the fallout of large drops formed on the seeded particles or the regeneration of the fog. The latter consists of a two-part process. Firstly, the vapor density of the foggy air is lowered below saturation long enough to evaporate some droplets below the critical size for their nucleus content. Secondly, when the fog is regenerated, the vapor density is forced to remain below the maximum value achieved during the initial, natural formation of the fog, and consequently fewer droplets grow beyond their critical radius. The result is fewer, larger drops and increased visibility. This regeneration process involves the introduction of a few additional, relatively large nuclei into the fog. The initial rapid growth of these nuclei causes the water-vapor pressure of fog to fall below saturation values, thus causing droplets having small nuclei to evaporate. It is necessary, however, to keep the water-vapor pressure below saturation for sufficient time to allow the droplets to evaporate to sizes smaller than the critical value associated with their nucleus.

Using the numerical model of liquid/vapor diffusion described in Koenig (1968) -- and summarized in Section III -- calculations were made of the time required to evaporate drops of differing nucleus content to their equilibrium sizes at supersaturations of -1 and -0.1 percent (subsaturated air). Figures 3 and 4 summarize these calculations, and show that substantial time is required to evaporate large fog droplets having small nuclei to a size below their critical radii -- even modest-sized drops require hundreds of seconds. As will be shown in Section IV, a seeded fog does not long remain greatly subsaturated, and subsaturations of about 0.1 percent may be regarded as representative of the subsaturated period of a successfully seeded cloud, if a method requiring a minimum of seeding material is used. Since rates of evaporation are approximately proportional to the degree of subsaturation, the time scale on the figures may be appropriately adjusted to suggest the evaporation at other subsaturations.

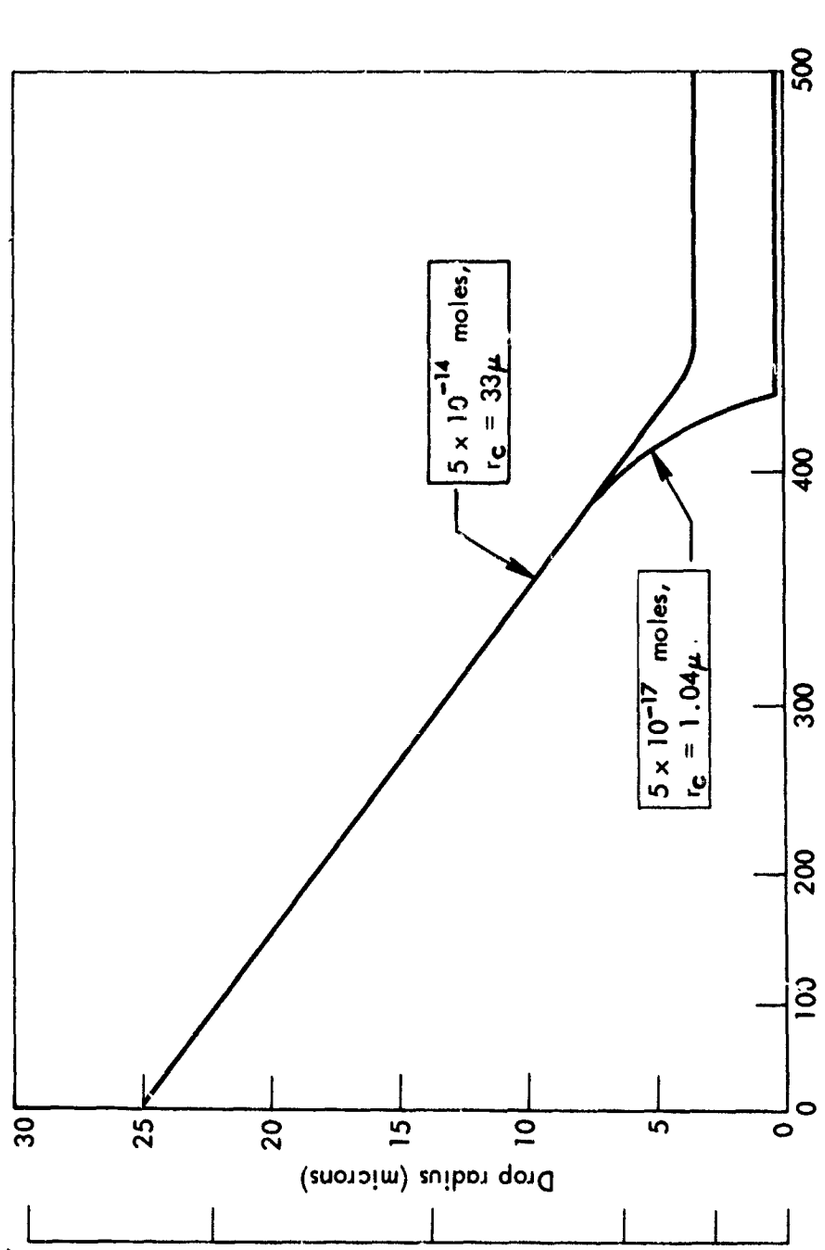

Fig. 3 -- Time required to evaporate drops containing various quantities of sodium chloride at supersaturation of -1%. (r_c is the critical size of the droplet.)

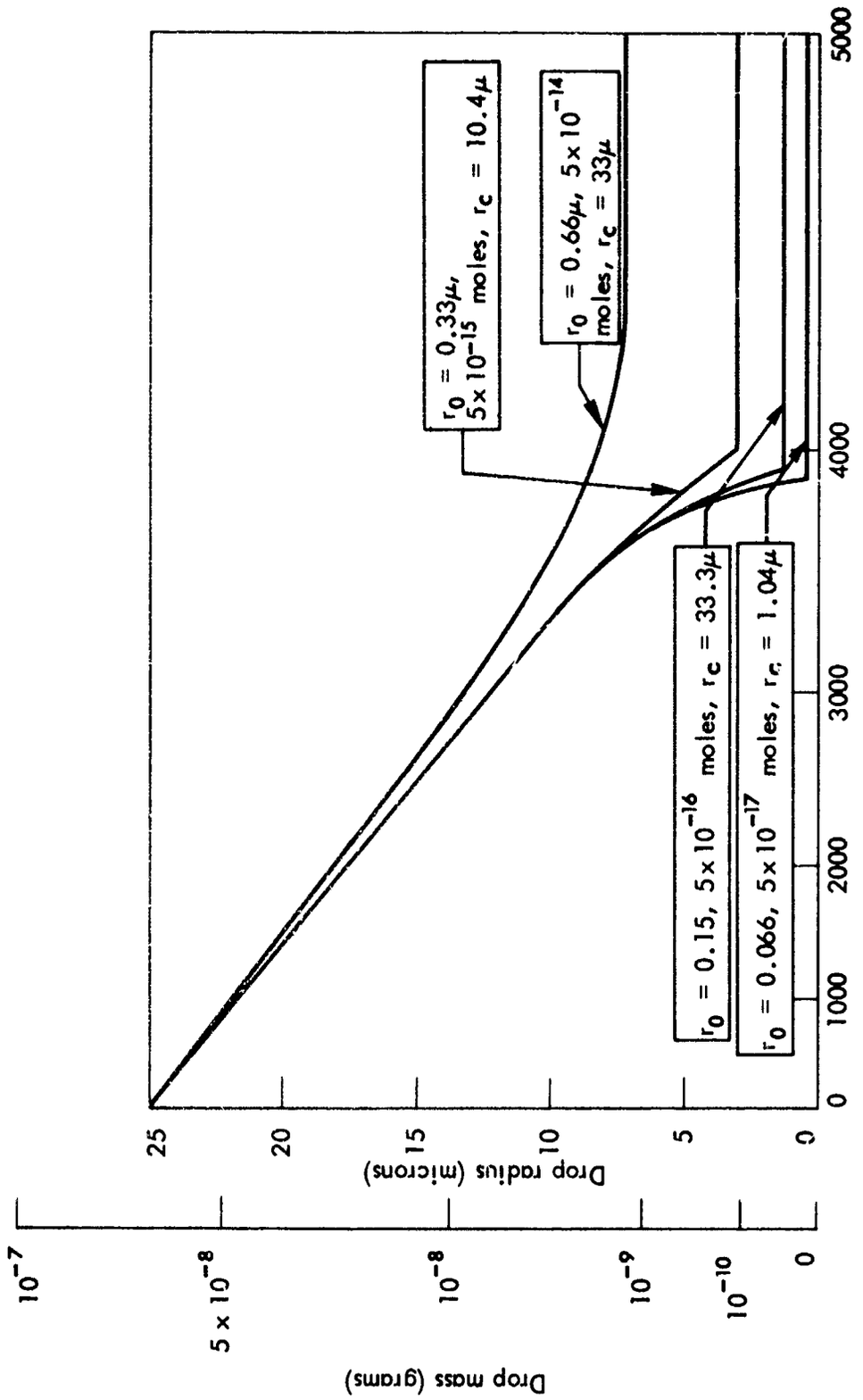

Fig. 4 -- Time required to evaporate drops containing various quantities of sodium chloride at supersaturation of -0.1%. (r_c is the critical size of the droplet, r_o the dry radius of the sodium chloride solute.)

Salt seeding lowers the water-vapor density below saturatio in a volume of foggy air by providing new centers of condensation whose equilibrium vapor pressure is lower than saturation, and that are numerous enough or large enough to absorb water from fog droplets in quantities sufficient to cause the droplets to evaporate below their critical radii. A measure of the ability of the seed drops to absorb water at the expense of fog particles is given by the size of the Raoult correction to the equilibrium vapor pressure over the seed droplet, or better, the virtual saturation, S_v, defined in Section III.

Using the numerical model, calculations were made to estimate the length of time that a seed particle remains effective in gaining water at the expense of other drops in the cloud. The results are shown in Figs. 5 and 6, where the virtual supersaturation over the seed particle and the growth of the seed droplet are shown as functions of time and of the ambient subsaturation. It is evident that if the seed particles must remain effective for periods of time greater than that required to evaporate fog droplets of moderate size, they must have a dry radius of at least 0.5μ, and in fact should be considerably larger. Smaller seed particles will only increase the number of droplets in the cloud and defeat the purpose of seeding.

An excess of seed particles will produce so many new droplets that they themselves materially reduce the visibility. However, if an insufficient number of seed particles is introduced, or if they are introduced too slowly, the ambient vapor pressure will not fall below subsaturation, and natural droplets will fail to evaporate. The same result will occur if seed particles are too small relative to the natural droplets.

We conclude that successful warm-fog seeding with condensation nuclei appears to require a technique that permits good engineering control over the size distribution, distribution rate, and ultimate concentration of the seed particles. Each of these parameters may be a function of the meteorological factors involved in the cooling process forming the fog and of the natural size distribution of condensation nuclei.

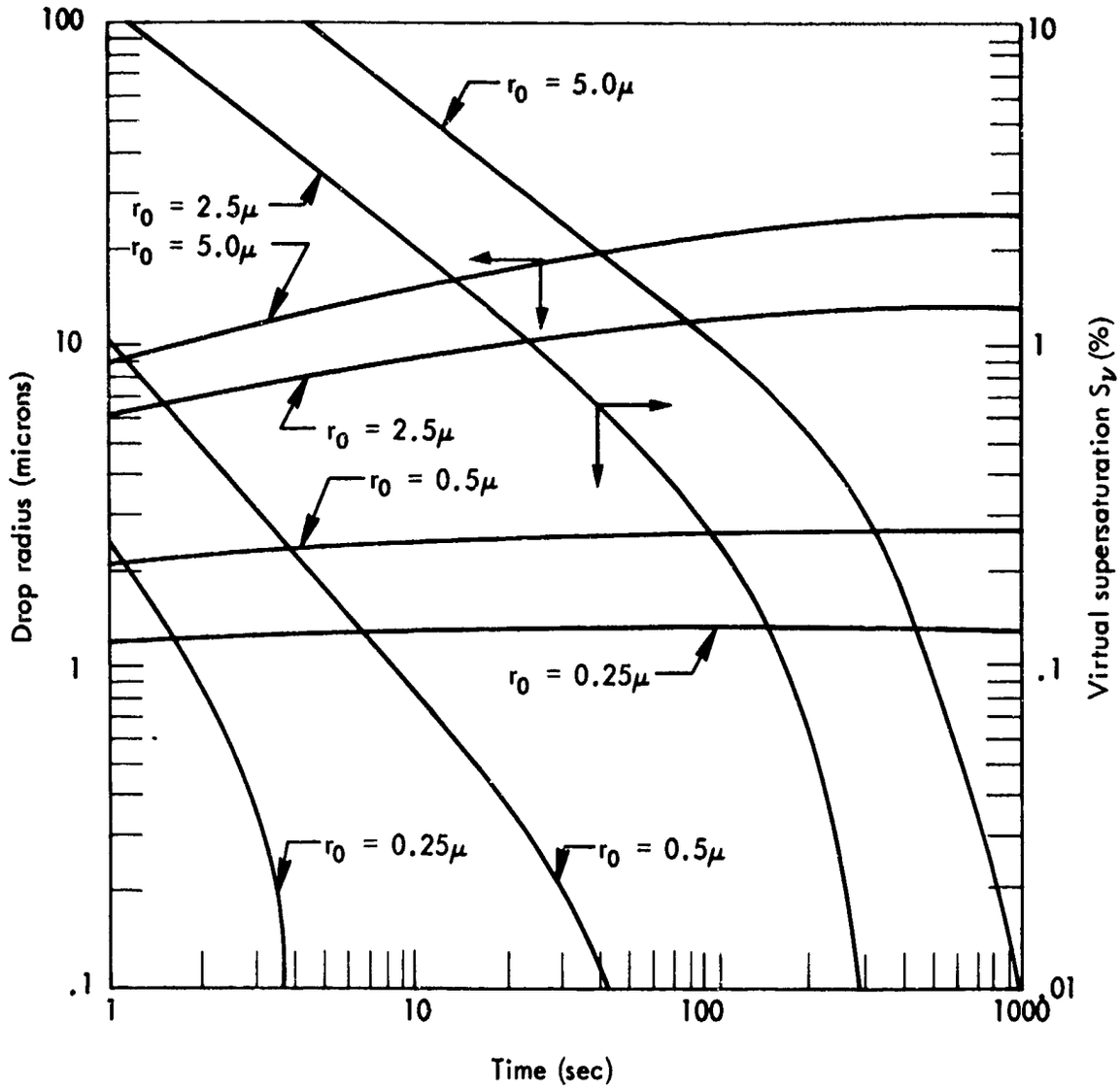

Fig. 5 -- Virtual supersaturation and drop radius as functions of time for droplets evaporating at supersaturation of -1.0% and containing various quantities of sodium chloride seed particles. (r_o is the dry radius of the sodium chloride solute; the relatively flat family of curves shows r versus t.)

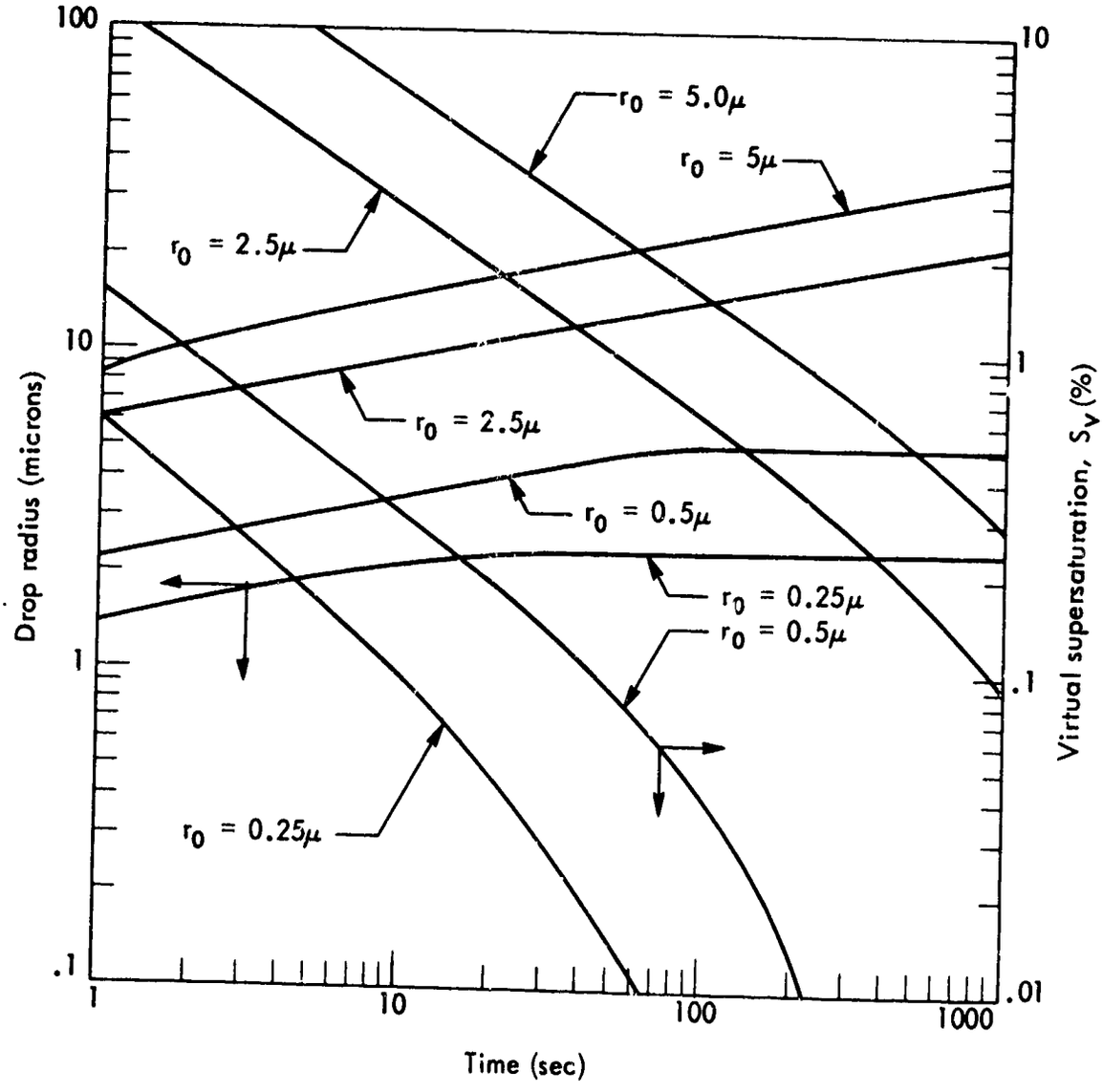

Fig. 6 -- Virtual supersaturation and drop radius as functions of time for droplets evaporating at supersaturation of -0.1% and containing various quantities of sodium chloride seed particles. (r_0 is the dry radius of the sodium chloride solute; the relatively flat family of curves shows r versus t.)

III. BASIS OF CALCULATIONS

CALCULATION OF TRANSPARENCY OF FOG

The goal of fog suppression is the improvement of an observer's ability to recognize objects. Recognition involves factors such as target characteristics and judgment, which lie outside the scope of meteorological phenomena and are thus excluded from consideration herein. For present purposes, the empirically definable term "meteorological range" will be equated with recognizability, and the measure of fog suppression achieved will be stated in terms of the improvement of meterological range one may predict as the result of simulated seedings. "Meteorological range" refers to the distance at which a large, stationary, black body appears to have a brightness contrast of 0.02 with respect to the horizon sky. A black body is an object that neither reflects nor radiates visible light. The physical bases for calculating meteorological range and the change in brightness contrast with distance from an object are discussed in this section. [A more thorough account may be found in Middleton (1952).]

The human eye responds to radiation having wave lengths between 0.4 and 0.7 microns, and has a maximum sensitivity to green light (between 0.5 and 0.57 microns). This is shown in Fig. 7, where Ψ_λ, the relative spectral luminosity, indicates the sensitivity or relative physiological response of the human eye to light of different wave lengths but of constant radiance (intensity). The monochromatic brightness (luminance), B_λ, of an object at a given wavelength is expressed by

$$B_\lambda = \Psi_\lambda I_\lambda \tag{3.1}$$

where I_λ is the intensity of the light incident on the eye.

The surface of a black body has (by the definition used here) a luminance of zero:

$$B \equiv \int_0^\infty B_\lambda d\lambda = 0 \tag{3.2}$$

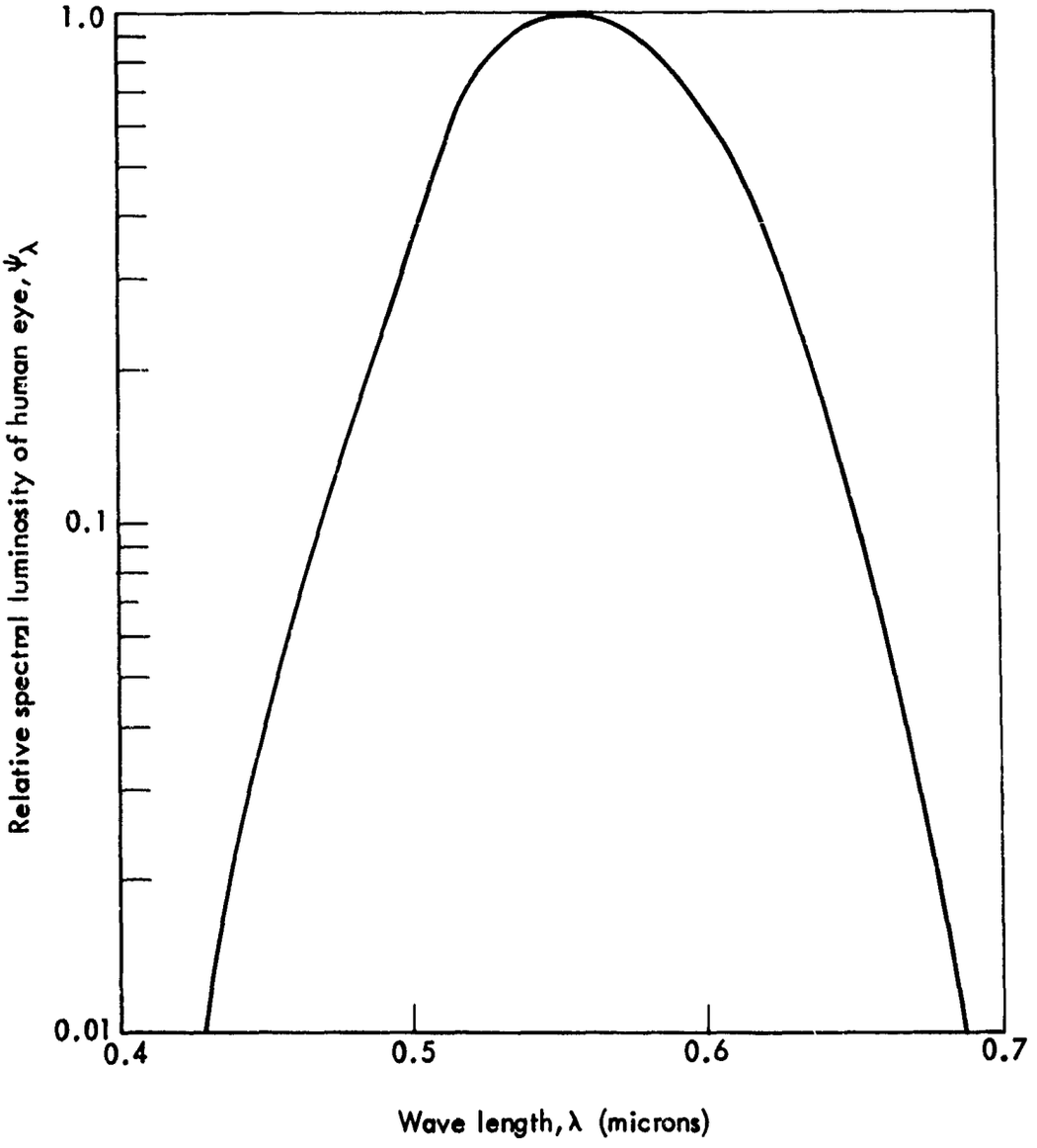

Fig. 7 -- Relative spectral luminosity (physiological response) of the human eye to light of different wavelengths (from List, 1966).

If the black object is observed in daylight at some distance from its surface, its apparent brightness will no longer be zero, since light is scattered by air molecules and aerosol particles into the line of sight of the observer. This superimposed scattered light appears to originate at the object, which thereby acquires an apparent brightness. The scattered light in the line of sight may itself be scattered and attenuated. The apparent brightness of the black object initially increases with distance, but if the distance becomes sufficiently large, the light gained by scattering into the line of sight will equal the light lost by attenuation and scattering out of the line of sight. Under this condition, brightness does not change with increasing distance, and the object will appear to have the same brightness as its background. Consequently, the contrast between object and background will vanish and the object will cease to be visable.

From Beer's Law, the brightness of an object (B_o) in relation to the sky or background brightness (B_s) may be expressed by

$$B_o = \int_0^\infty B_{s\lambda}\left(1 - e^{-\sigma_\lambda x}\right)d\lambda \tag{3.3}$$

where x is the path length through the uniform scattering volume and σ_λ is the monochromatic extinction coefficient

$$\sigma_\lambda = n\pi K_{s\lambda} r^2 \tag{3.4}$$

It is the dependence of the extinction coefficient on the concentration (n) and radius (r) of the droplets in the scattering volume that results in brightness being a function of the micro-physical properties of fog. The effects of scattering and attenuation by air molecules on the extinction coefficient are not considered in this work, since these are comparatively small in fog.

The extinction coefficient is also a function of wavelength, owing to the dependence of the value of the scattering-area coefficient, $K_{s\lambda}$, on the wavelength of the light involved. This dependence is shown in Fig. 8, where smoothed values of K_s are plotted against ratios of the drop radius to the wave length of radiation. Figure 9 is a modification of Fig. 8, and is designed to show more explicitly the dependence of K_s on drop size. In Fig. 9, $\bar{K}_s$ is plotted against drop radius, using for each drop size a weighted value based on the spectral sensitivity of the eye (Ψ_λ), shown in Fig. 7, and the spectral distribution of the intensity of sunlight at the top of the earth's atmosphere, shown in Fig. 10. Values of $\bar{K}_s(d)$ were calculated from

$$\bar{K}_s(d) = \frac{\sum_{\lambda=0.4\mu}^{\lambda=0.7\mu} K_s(d)_\lambda \Psi_\lambda I_\lambda}{\sum_{\lambda=0.4\mu}^{\lambda=0.7\mu} \Psi_\lambda I_\lambda} \tag{3.5}$$

As revealed in Fig. 9, drops with a diameter larger than about 5μ have scattering-area coefficients that are essentially independent of drop size and equal to 2. For smaller droplets, $\bar{K}_s$ is a rapidly varying function of drop size. On the basis of our assumption that most of the decreased visibility in fog is caused by droplets larger than 5μ in diameter, we used a constant value (equal to 2) of K_s.*

If K_s is constant and independent of wave length, then the extinction coefficient is also independent of wave length, and may be simplified to

$$B_o = B_s(1 - e^{-\sigma x}) \tag{3.6}$$

*In retrospect, it appears that these assumptions merit further examination.

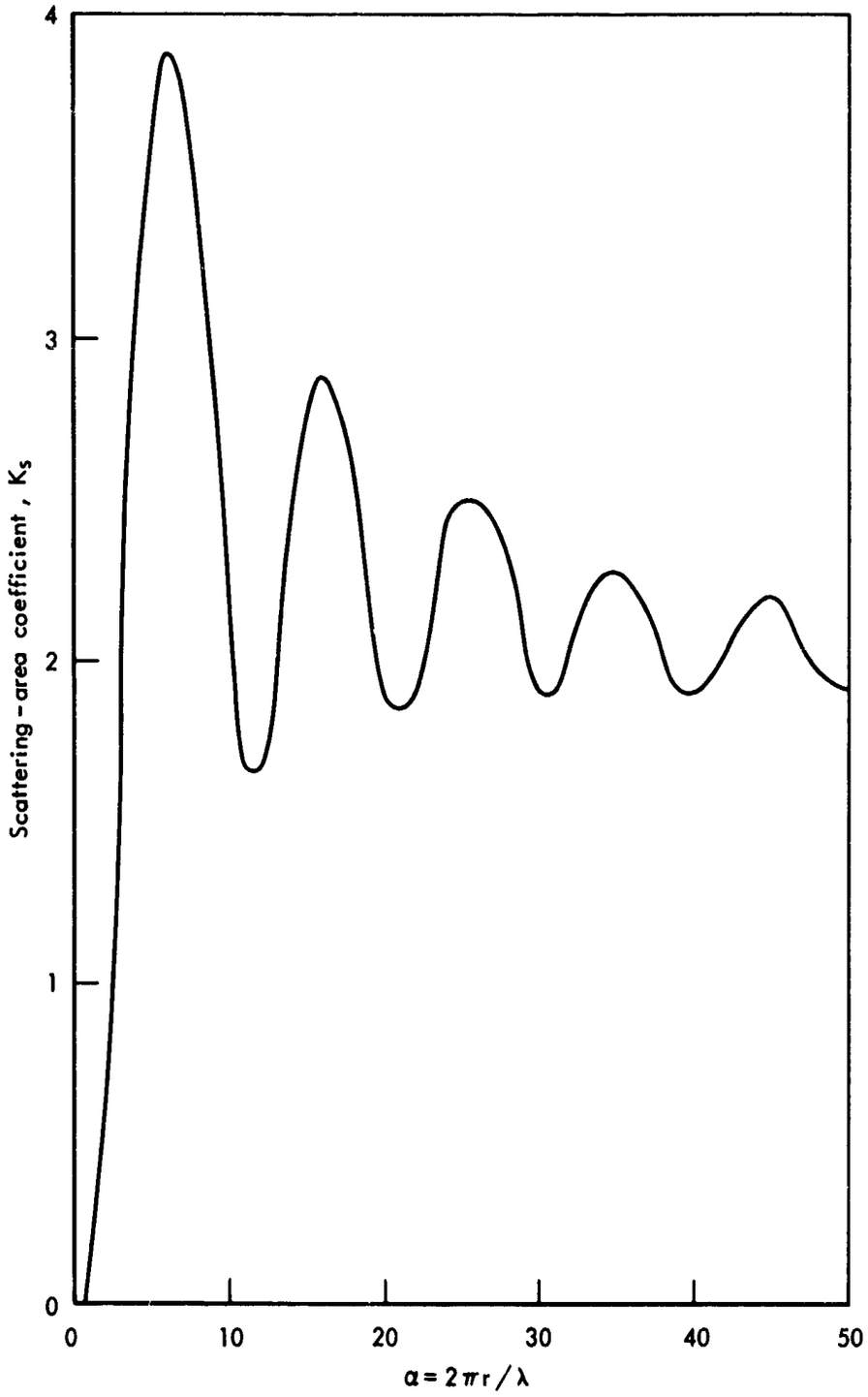

Fig. 8 -- Smoothed curve of the variation of scattering-area coefficient with function of drop size and wavelength of light (from List, 1966).

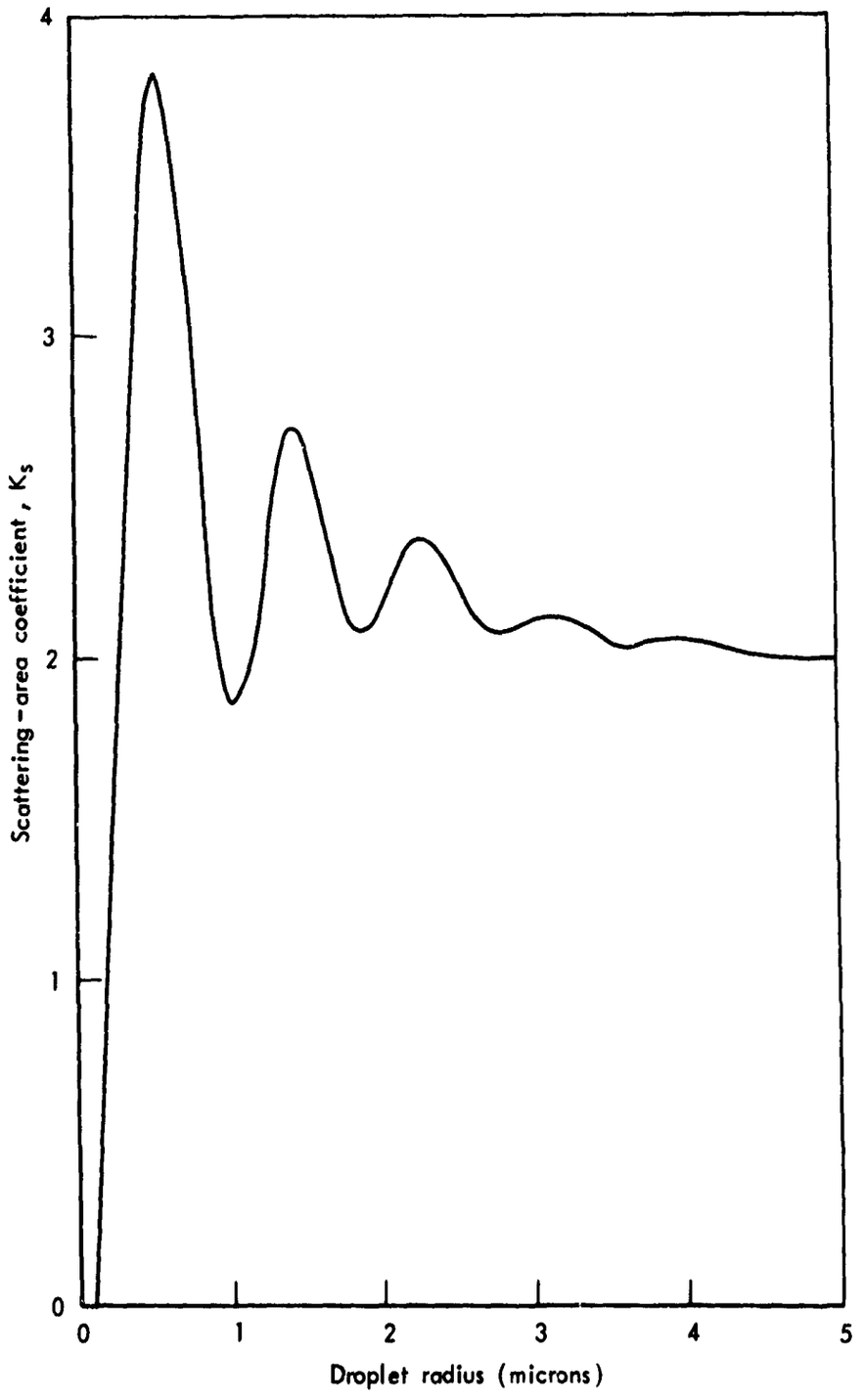

Fig. 9 -- Smoothed curve of the variation of scattering-area coefficient with drop size, using weighted value of light based on the spectral composition of sunlight and the physiological response of the human eye.

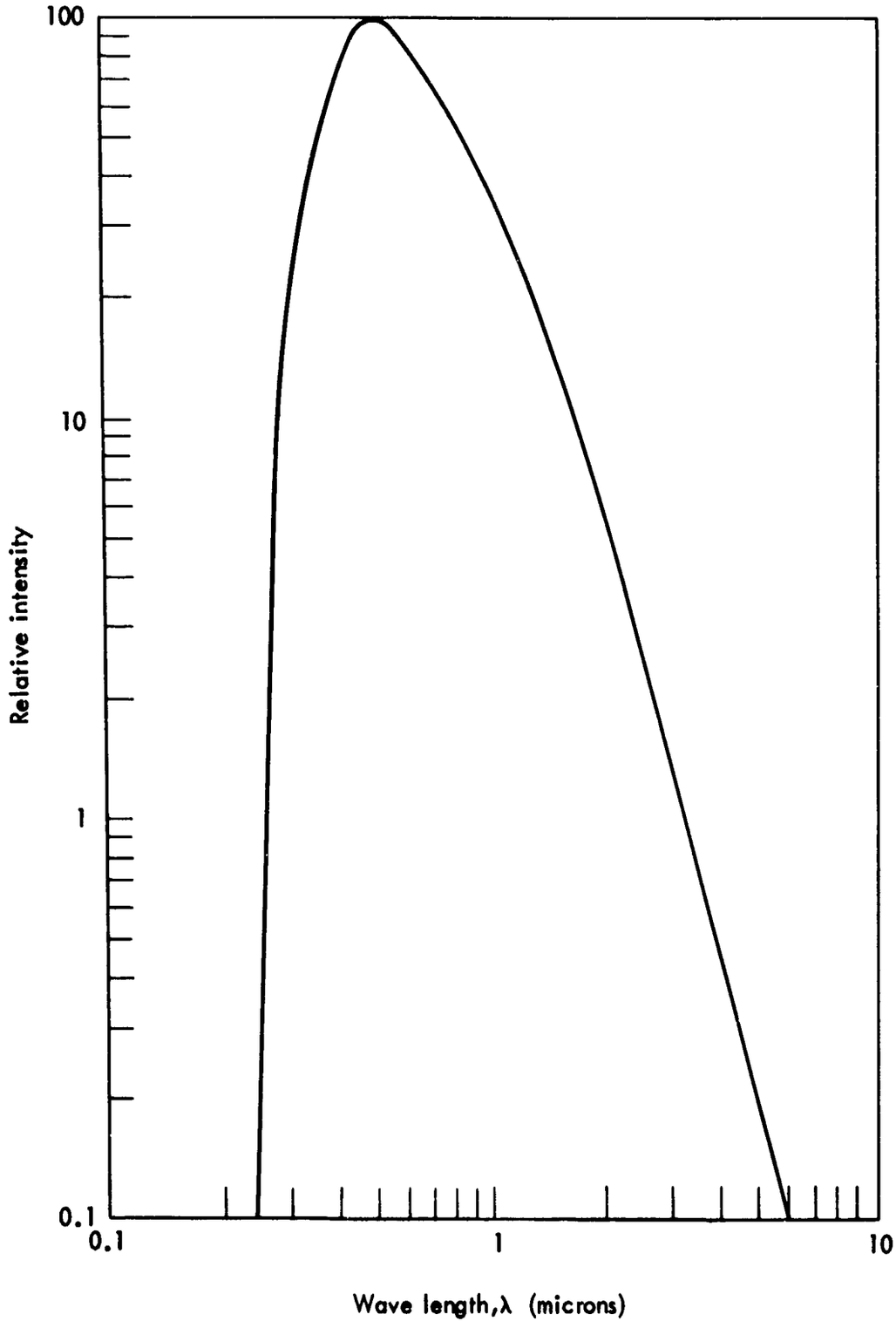

Fig. 10 -- Spectral distribution of sunlight at the top of the earth's atmosphere (from List, 1966).

The brightness contrast (C) of an object against its surroundings is defined as

$$C \equiv \frac{B_o - B_s}{B_s} \tag{3.7}$$

Equation (3.6) may then be substituted into Eq. (3.7) to yield

$$C = e^{-\sigma x} \tag{3.8}$$

The threshold of brightness contrast of the human eye depends on many factors. For comparative purposes a value of ±0.02 is often used, and has been adopted to specify the meteorological range. Calculations of the "visual range" should make use of the prevailing threshold of brightness contrast; however, a value of ±0.02 is often used, and in this case "visual" range and "meteorological" range are synonymous. Using a value of 0.02 in Eq. (3.8), we obtain

$$e^{\sigma x_r} = 0.02 \tag{3.9}$$

Taking logarithms,

$$x_r = \frac{3.912}{\sigma} \tag{3.10}$$

or

$$x_r = \frac{3.912}{\sum_{i=0}^{i=\infty} n_i K_s \pi r_i^2} = \frac{0.6226}{\sum_{i=0}^{i=\infty} n_i r_i^2} \tag{3.11}$$

Equation (3.11) forms the basis of the method of calculating meteorological range used in this report.

CALCULATION OF DROPLET EVOLUTION

The foundation of our present predictions of droplet evolution is the numerical model of condensation described by Koenig (1968). The "less complex" model described in the cited report was used in the present work. Briefly, mass-transfer rates are calculated in that model from the expression

$$\frac{dr}{dt} = \frac{\left[e_\infty - (e_s^*)_{T_\infty}\right] \Big/ (e_s^*)_{T_\infty}}{r\rho_w \left[\frac{JL^2 M_w}{KRT_\infty^2} + \frac{RT_\infty}{DM_w(e_s^*)}\right]} \tag{3.12}$$

In this expression, $(e_s^*)_{T_\infty}$ is the saturation vapor pressure over the drop if it is neither growing nor evaporating; it takes into account the drop's size and molality, but assumes that it is at ambient temperature. The value of $(e_s^*)_{T_\infty}$ is found by Teten's formula (Murray, 1967), modified for the effects of molality and size by Raoult and Kelvin corrections:

$$(e_s^*)_{T_\infty} = 6107.8 \exp\left[\frac{17.269388\ (T_\infty - 273.16)}{(T_\infty - 35.86)}\right] \text{ (Teten's formula)}$$

$$\times \frac{1}{1 + i m_n M_w / M_n m_w} \text{ (Raoult correction)} \tag{3.13}$$

$$\times \exp\left(\frac{2\tau M_w}{T_\infty R r \rho_w}\right) \text{ (Kelvin correction)}$$

The concept of "virtual supersaturation" used in this Memorandum is an approximate expression of the driving force causing a drop to grow, whereas "true supersaturation" is an approximate expression of the driving force causing mass transfer across a pure, flat water surface. The former is defined as

$$S_v = \frac{e_\infty - (e_s)_{T_\infty}}{(e_s^*)_{T_\infty}} \qquad (3.14)$$

THE FOG MODEL

For the fog model used in this work, a spectrum of aerosol particles was input, and the growth rate of each particle was computed using Eq. (3.12). Air temperature and pressure may also be input variables, but in the work reported, pressure was always 1000 mb and the air was initially at water saturation. A fixed temperature decrease with time was usually assumed; however, a draft velocity may be specified to account for the air cooling necessary for fog formation. In the former case, the feedback effects of the release of the latent heat of condensation on the air temperature may either be taken into account (to modify the assigned temperature drop) or ignored. When the draft velocity was specified, this feedback was always taken into account.

To calculate the virtual supersaturation for each nucleus, $(e_s^*)_{T_\infty}$ was calculated and a trial-and-error iterative procedure was used to calculate the ambient water-vapor pressure (e_∞) and supersaturation. In this procedure, e_∞ was initially estimated on the basis of the temperature drop between time steps and the excess water-vapor pressure over saturation from the previous time step. The first estimate of e_∞ was used to calculate mass transfer to the entire population of droplets. The ambient supersaturation before the time step was compared with that after the time step, the temperature drop and transfer of water from the air to the droplets being considered. If the supersaturations before and after the step agreed within specified limits, it was assumed that a satisfactory value of e_∞ had been used, and the calculation was continued. This procedure resulted in a smooth change in the water-vapor density of ambient air and held the water-vapor density excess (or deficit) with respect to saturation reasonably constant between time steps, but allowed longer-term changes. Euler integration was used with time steps of 10 seconds.

Droplet fallout was incorporated into the model. Before each time step, a uniformly mixed cloud was assumed. The terminal velocity of each drop was calculated on the basis of the data of Gunn and Kinzer (1949), and the loss of drops (Δn_j) by fallout at the end of the time step was calculated by

$$\Delta n_j = n_j \times \frac{V_j}{d} \tag{3.15}$$

IV. RESULTS

VERIFICATION OF THE NUMERICAL MODEL

The validity of the numerical model was checked by comparing its predictions with experiments conducted at the Cornell Aeronautical Laboratory (Pilié et al., 1967; Juisto et al., 1968). These experiments were conducted in a cylindrical chamber 9 m high and 9 m in diameter. Fog was formed on natural aerosol nuclei in the atmosphere by first pressurizing the chamber and then cooling the air by venting the chamber in a controlled manner. No cooling occurred between 8 and 11 minutes, the period in which seeding was accomplished. Visual range was calculated from measurements of the extinction coefficient obtained with a transmissometer. The seeding agent used was sodium chloride.

A run using an 8-mg/m^3 NaCl seeding agent having a maximum particle number concentration between 4 and 5μ in diameter is discussed in some detail in the Cornell reports, and is used herein as the principal basis of verification of the model. In our numerical experiment, the distribution of the natural aerosols was simulated by means of 27 particle sizes, peaked at 0.1μ in diameter (Table 1). The size-distribution of seed particles was simulated by 5 particle sizes (Table 2), and approximates the distribution given by Juisto et al. (1968).

A cooling rate of 4°C/hour from an initial temperature of 24°C was reported by the Cornell experimenters. A comparison of the laboratory and numerical experiments is shown in Fig. 11. The reported values of liquid water density within the laboratory-produced fog are considerably smaller than either those predicted in the numerical model or those resulting in adiabatic cooling of 4°C/hour with no fallout of cloud droplets. If the Cornell experiments were made using an expansion rate for which the dry adiabatic cooling rate would be 4°C/hour, the cooling rate with concurrent condensation would be about half that value (because of warming due to heat of condensation). If a cooling rate of 2°C/hour is assumed, the computed liquid water density approximates those measured during the Cornell experiments, and experimental results and numerical calculation are in even closer agreement

Table 1

AEROSOL DISTRIBUTIONS USED IN EXPERIMENTS

Diameter of Dry Nucleus (microns)	0.10μ Peak		0.35μ Peak
	No. per cm^3 if total$_3$= 500/cm^3	Relative concentration (%)	Relative concentration (%)
0.05	18.59	3.585	0.024
0.06	27.89	5.578	0.048
0.07	37.19	7.438	0.097
0.08	46.49	9.298	0.145
0.09	55.78	11.155	0.193
0.10	74.38	14.875	0.242
0.12	55.78	11.155	0.483
0.14	46.49	9.298	0.967
0.16	37.19	7.438	1.450
0.18	27.89	5.578	1.93
0.20	18.59	3.718	2.417
0.22	9.30	1.860	4.835
0.24	8.37	1.674	7.252
0.26	7.44	1.488	9.670
0.28	6.51	1.302	12.087
0.30	5.58	1.116	14.505
0.35	4.65	0.930	19.340
0.40	3.72	0.744	14.505
0.50	2.79	0.588	4.835
0.60	1.86	0.372	1.934
0.70	0.930	0.186	0.967
0.80	0.837	0.167	0.483
0.90	0.744	0.149	0.242
1.50	0.930	0.186	1.209
2.50	0.0930	0.019	0.121
3.50	0.00930	0.0019	0.0121
4.50	0.000930	0.0019	0.00121

Table 2

SEED SIZE DISTRIBUTION USED
IN SIMULATING THE CORNELL EXPERIMENT

Diameter of Dry Seed Particles (microns)	Relative Concentration (percent)
1.0	12.0
2.0	15.0
3.0	14.0
4.0	19.0
5.0	15.0
6.0	10.0
7.0	7.0
8.0	3.0
9.0	5.0

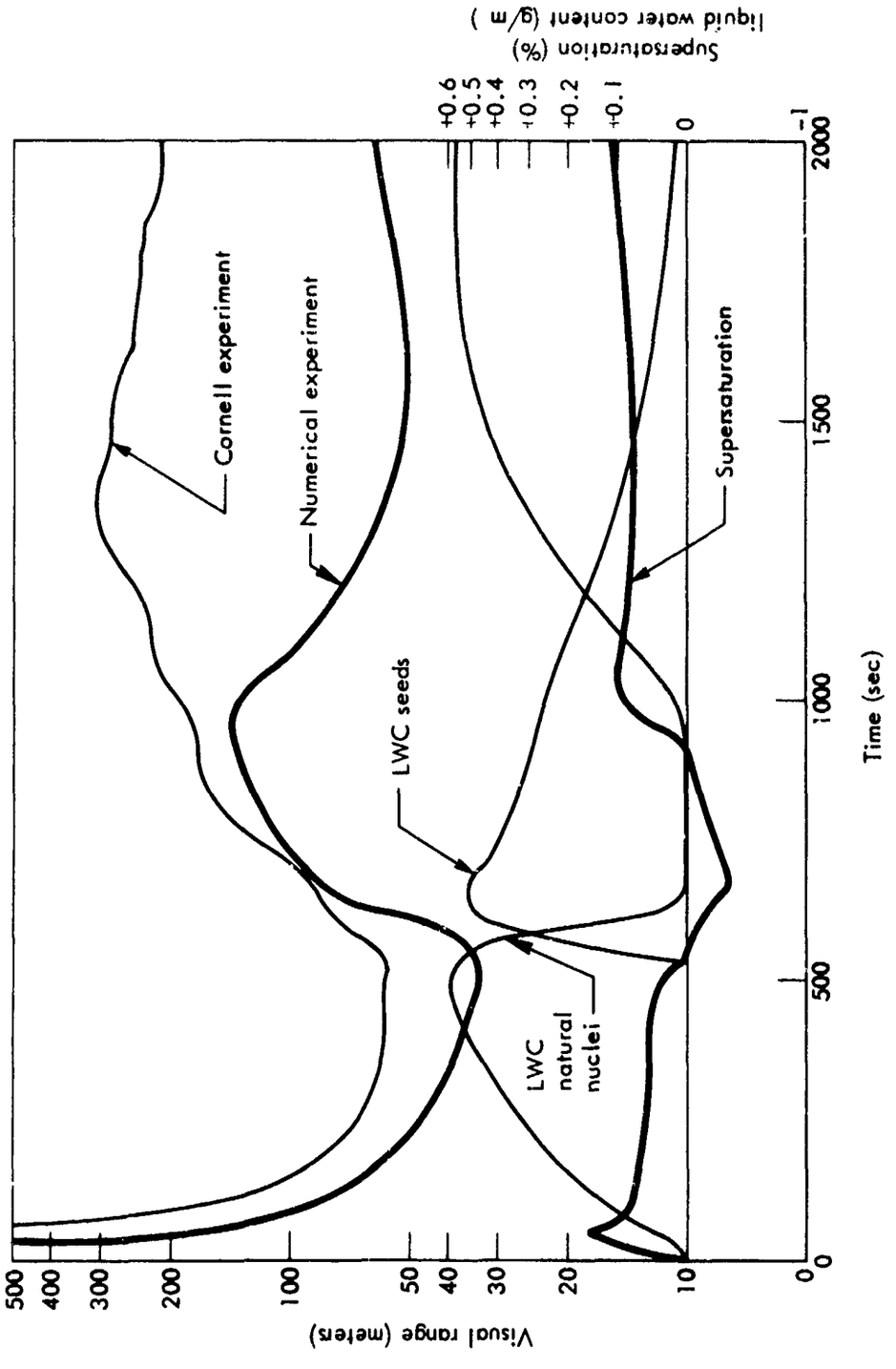

Fig. 11 -- Comparison of visual (meteorological) range from laboratory data (Cornell Aeronautical Laboratory) and numerical model; cooling rate, -4°C/hour. Lower curves show trend of supersaturation and liquid water content (LWC). Cloud 9m thick.

with respect to visibility and visibility improvement (Fig. 12). The distribution of water density between natural and seed particles is shown in Figs. 11 and 12, and the change of fog-droplet size distribution with time is shown in Fig. 13.

Although numerical simulation and laboratory experiment are not in particularly good agreement if the stated 4°C/hour cooling rate is used in the numerical calculation, there seems to be sufficient justification to compare visibility and visibility-improvement factors under the assumption of a 2°C/hour cooling rate. If this is done, there is good agreement between laboratory and numerical experiments. If lesser amounts of seeding materials are simulated, visibility improvement decreases in accordance with experimental observations.

Figures 11 and 13 illustrate the characteristic simulated behavior of fog during seeding. Initially the dry aerosol particles absorb water and become larger; a peak in supersaturation occurs shortly after the relative humidity exceeds 100 percent (~50 sec in Fig. 11). After this peak supersaturation is reached, the aerosol spectrum can be regarded as dividing itself into two groups: (1) larger aerosols upon which stable fog droplets form and continue to grow, and (2) smaller aerosols which cease growing and remain haze-size particles. The latter particles never reach the critical size and supersaturation corresponding to their nucleus content. In Fig. 13a, the absence of particles of from 1 to 5μ in diameter indicates that droplets incorporating natural aerosols segregate into "haze particles" (smaller than ~3μ) and "fog droplets" (larger than ~3μ).

As time passes, both visibility and supersaturation decrease, while fog droplets grow larger and the liquid-water content increases. The number density of drops diminishes slightly, primarily because larger drops tend to fall out. Shortly after seeding (~600 sec in Figs. 11 and 13), the relative humidity falls below 100 percent, and many of the fog droplets evaporate to the size of haze particles. Consequently, the liquid-water content of droplets incorporating natural aerosol particles rapidly decreases, while that of seed-containing droplets increases. Although the total number of fog-size droplets decreases, the spectrum of sizes broadens and visibility improves.

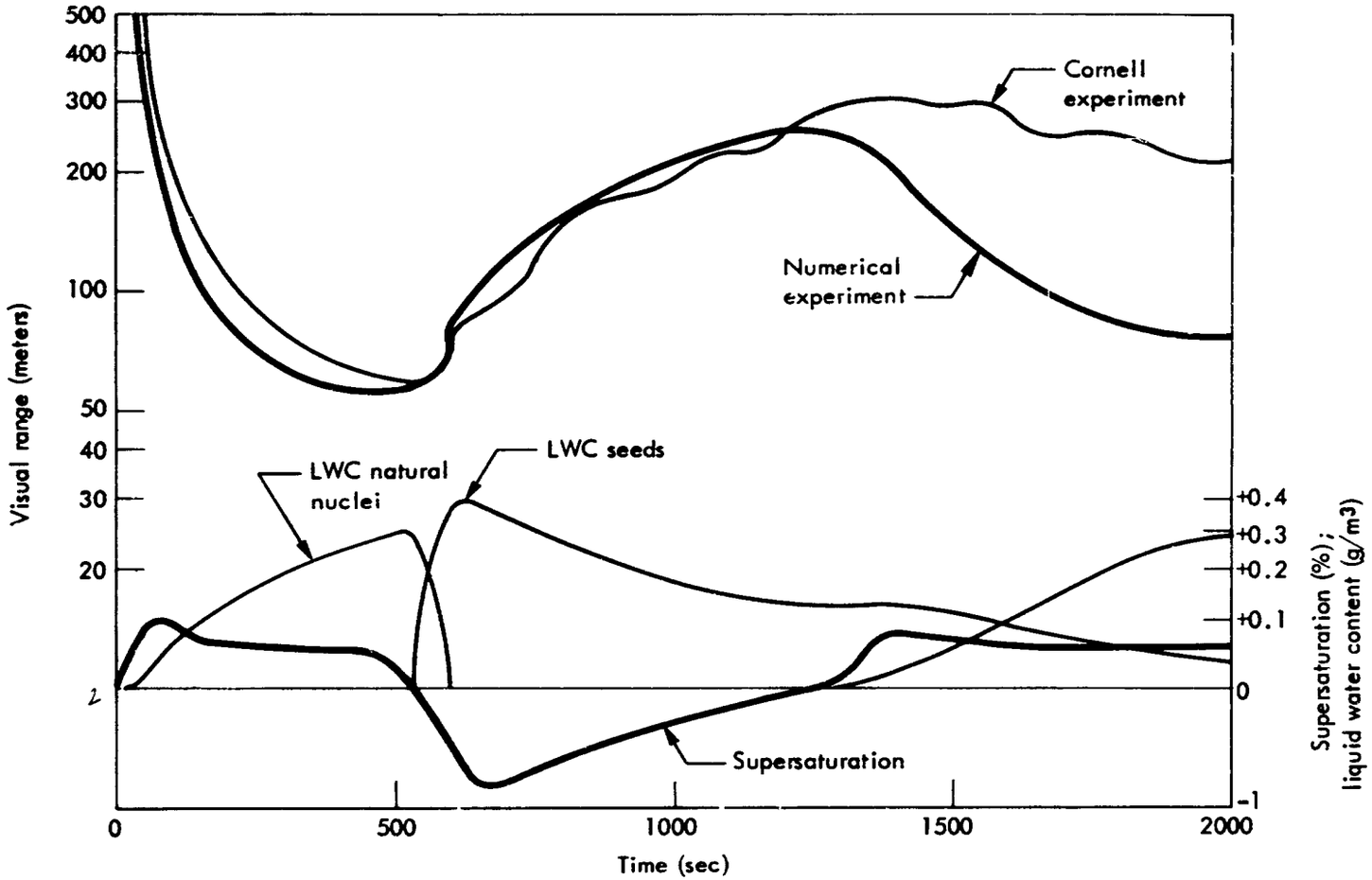

Fig. 12 -- Comparison of visual (meteorological) range from laboratory data (Cornell Aeronautical Laboratory) and numerical model; cooling rate, -2°C/hour. Lower curves show trend of supersaturation and liquid water content (LWC). Cloud 9m thick.

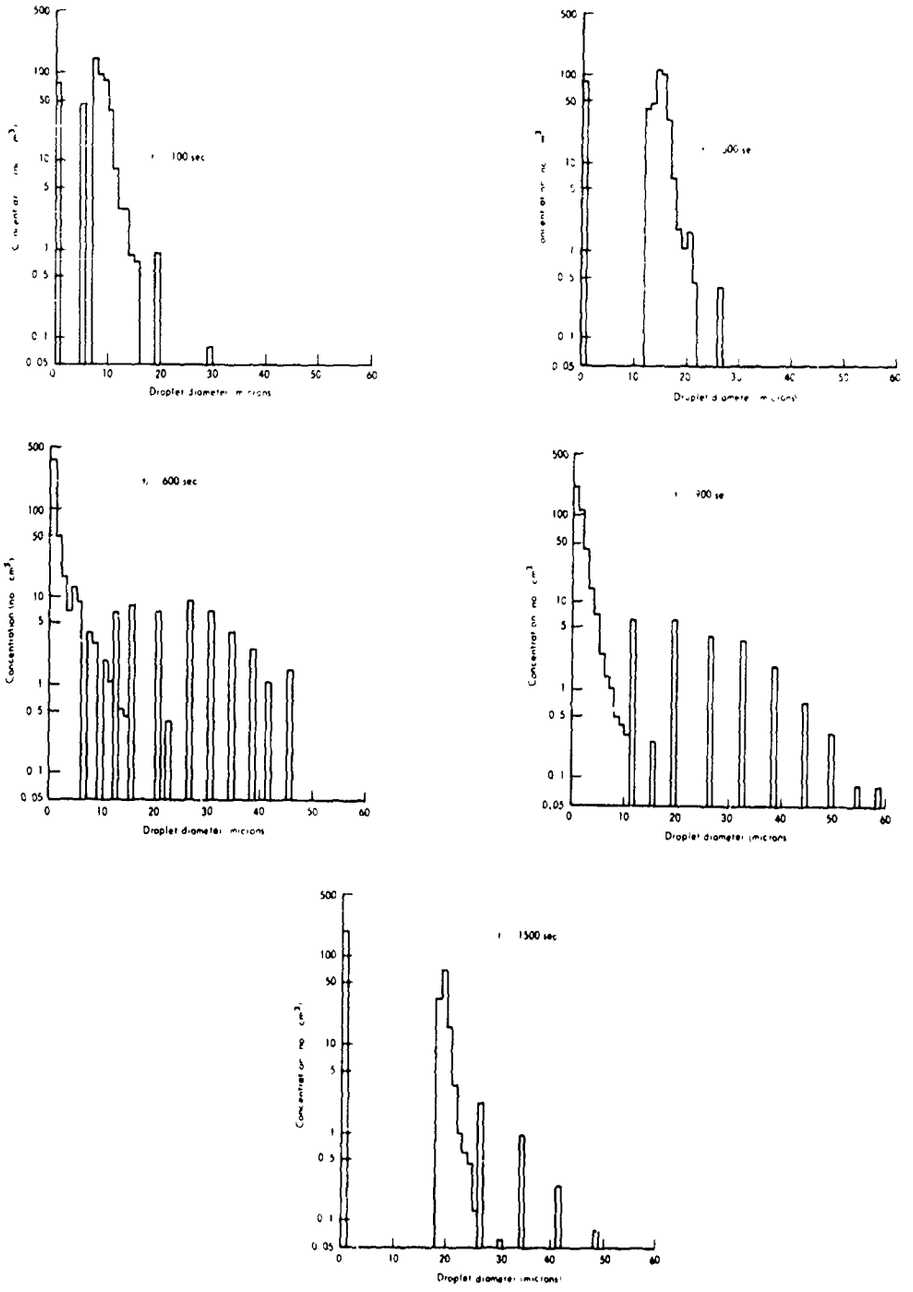

Fig. 13 -- Change in fog-droplet size distribution with time, predicted by numerical model using 8mg/m^3 sodium chloride seeding agent and cooling rate of -4°C/hour. Cloud 9m thick.

The ability of the seed material to absorb water continually decreases, firstly because the seed-containing droplets become dilute and the vapor density over them approaches that of infinitely dilute droplets, and secondly, because the larger, seed-containing droplets fall out of the fog.

Ultimately the improvement in visibility reaches a maximum. At this time (~900 sec in Figs. 11 and 13) the relative humidity has increased to approximately 100 percent, and many of the original aerosol particles are once again growing to fog-droplet size. There is still a broad size-distribution of particles, but most large seed particles have fallen out, removing a significant quantity of water -- an important source of visibility improvement.

Visibility continues to decrease as the original aerosol particles grow to fog-droplet size, the number density of droplets increases, and once again most of the liquid-water content of the fog is found in drops containing the original aerosol particles. One can consider the fog as once more established and unaffected by the seeding operation. It is noteworthy that in the second generation of fog, both a peak supersaturation and a break between haze particles and fog droplets occur, just as during the original formation of fog.

The above sequence of events is similar to that observed in the Cornell experiments, except that the fog is re-established more quickly in the numerical simulation. We conclude that the numerical simulation represents the experimental findings sufficiently well to justify additional numerical experiments and the assessment of ranges of applicability of salt seeding.

All the simulation experiments performed with the model incorporated a thermal sequence similar to that of the Cornell experiment: initial cooling from saturation for about 9 minutes, followed by isothermal seeding for about 3 minutes, followed by cooling. Hence, conditions conducive to continual fog generation were present after seeding, and visibility improvement underwent subsequent deterioration as the effectiveness of the seeded material declined with time. At present, for out-of-doors operations, it seems premature to attempt to disperse an actively forming fog, as modeled above. It would be more

practical rather to hasten the departure of a stagnant or slowly dissipating fog. If continual cooling (fog generation) were excluded from the experiments, one would expect a continual improvement in visibility, owing to the continual fallout of droplets and the resultant lowering of the liquid-water content of the fog, even after all seed material loses its potency. Of course, turbulent mixing of unaffected fog-bearing air from the surroundings will continually act to decrease visibility.

EFFECT OF SEED QUANTITY

Table 3 summarizes the results of calculations whose mutual comparison sheds light on the effect of seed quantity upon visibility improvement. Figure 14 illustrates predicted seeding results with three different quantities of seed and a constant cooling characteristic, initial aerosol spectrum, and seed size. Similar data from experiments with larger seeds and greater cloud depth are shown in Fig. 15. These results indicate there is an optimum quantity of seed. Too few seeds (e.g., 2 mg/m^3 in Fig. 14) result in little visibility improvement, for the capacity of the seeds to absorb water from the natural fog particles is too small, and the water-vapor density does not fall below saturation long enough or far enough to cause the natural fog droplets to evaporate to haze-particle size. If the seeds lose their effectiveness too quickly, water-vapor saturation becomes positive and the natural particles resume their growth. Too many seeds, on the other hand, although providing a long period of time during which the water-vapor density is below saturation (e.g., 27 mg/m^3 in Fig. 15) result in little visibility improvement. In effect, one has only replaced droplets formed on natural nuclei with those formed on seeded nuclei. It should be borne in mind that since seeding lowers the ambient water-vapor density, water vapor is converted to liquid water, and in the absence of fallout the liquid-water content of the fog increases.

If there is no substantial fallout or redistribution of liquid water into fewer, bigger drops, no clearing occurs. For effective clearing, it is necessary to reduce the number of fog droplets; this

Table 3

INFLUENCE OF SEED QUANTITY AND SIZE ON VISIBILITY IMPROVEMENT[a]

Simulated Condition				Visual Range		Time at Max. Visual Range (sec)	Ratio Visual Range (max/min)
	Seed Parameter						
Cloud Depth (meters)	Diameter (microns)	Mass (mg/m^3)	Concentration ($No./cm^3$)	Minimum (m)	Maximum (m)		
9	5	2	14.2	33	44	800	1.3
9	5	4	28.5	33	97	900	2.9
9	5	8	57.0	29	160	1,110	5.5
90	5	1	7.1	29	34	640	1.2
90	5	2	14.2	29	31	680	1.1
90	5	4	28.5	29	55	920	1.9
90	5	8	57.0	29	52	680	1.8
90	10	12	10.6	29	100	1,300	3.4
90	10	16	14.0	29	97	1,500	3.3
90	10	27	24.0	29	91	2,000+	3.1+
90	20	32	3.5	29	256	1,150	8.8
90	20	64	7.0	29	307	1,580	10.6
90	40	32	0.44	29	39	760	1.3
90	40	64	0.88	29	373	960	12.8
90	80	32	0.054	29	31	670	1.1
90	80	512	0.88	29	24,700	1,490	850.0[b]

[a]All runs were with 500 natural aerosol particles/cm^3 and a peak concentration at 0.1μ diameter; cooling rate was 4°C/hr.

[b]See comment in text under heading "Effect of Seed Size."

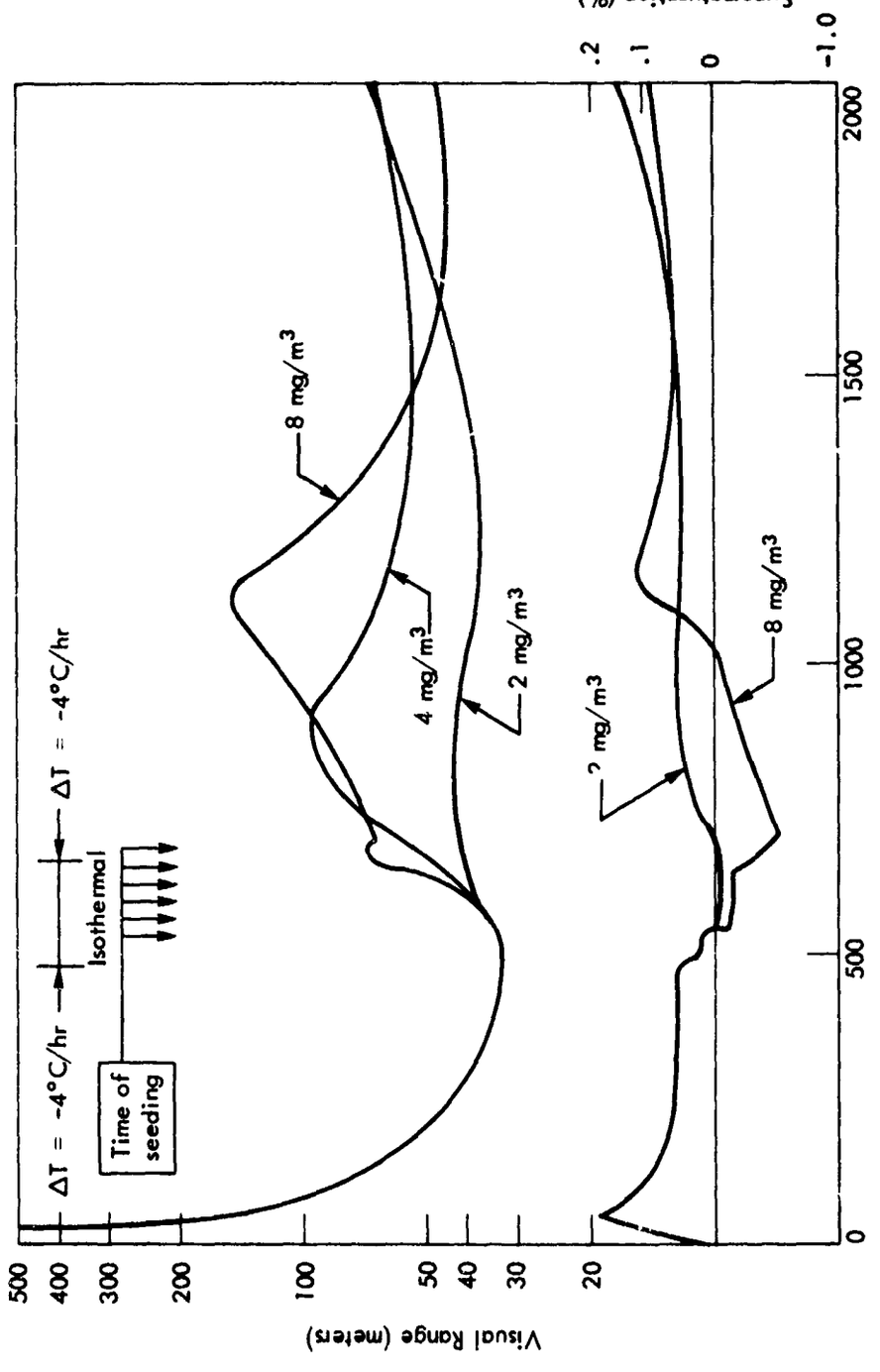

Fig. 14 -- Comparison of predicted change in visual (meteorological) range with time, using several seeding rates. Seed particles 5μ in diameter; original aerosol contained 500 particles/cm^{-3} peaked at 0.1μ diameter; cooling rate, -4°C/hour. Cloud 9m thick.

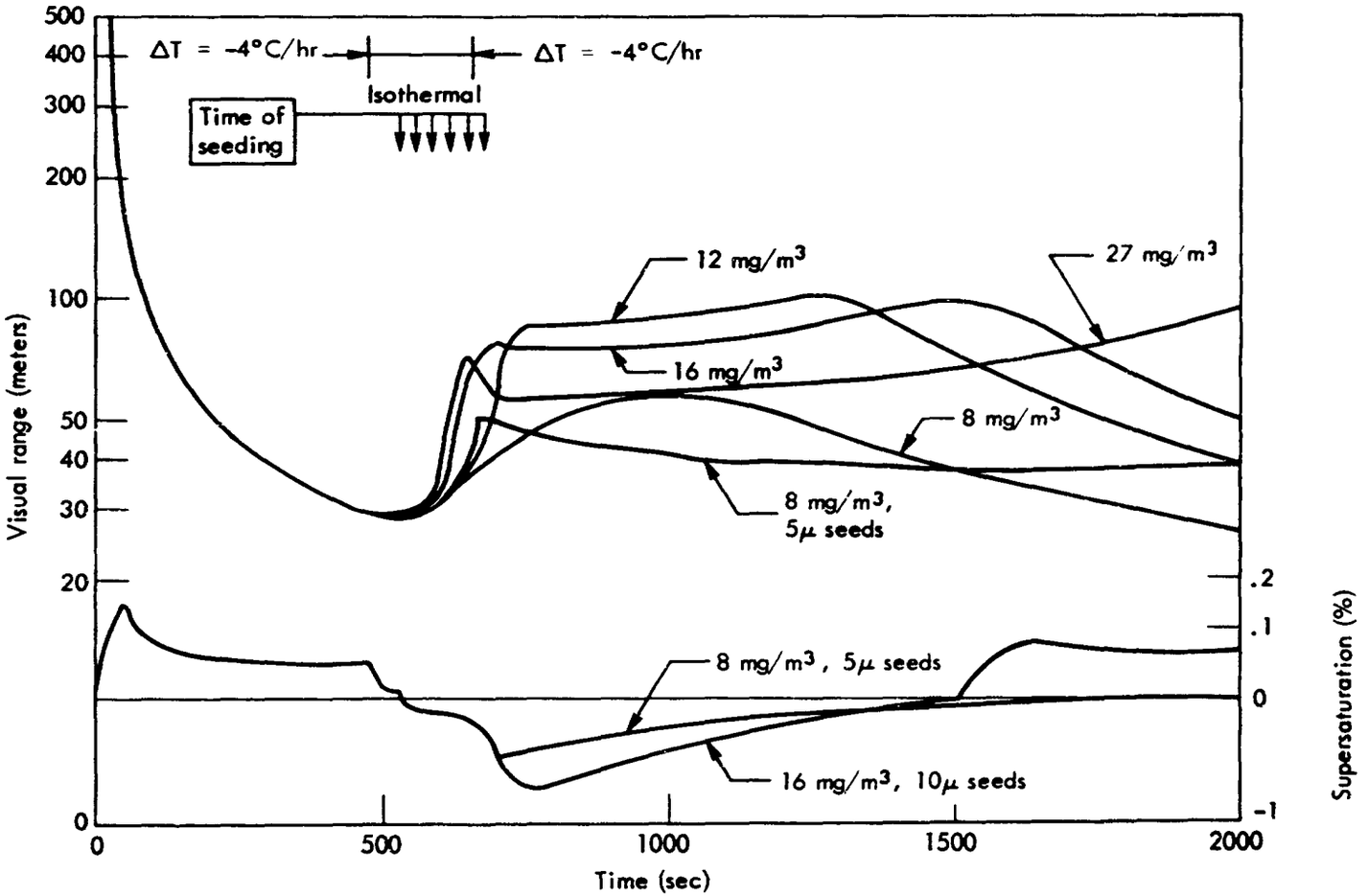

Fig. 15 -- Comparison of predicted change in visual (meteorological) range with time, using several seeding rates and seed sizes (seeds 10μ in diameter except where noted). Original aerosol contained 500 particles/cm^3 peaked at 0.1μ diameter; cooling rate, -4°C/hour. Cloud 90m thick.

implies that one must limit the concentration of seed particles regardless of their size.

The ideal concentration of seed is a function of seed size and cloud depth. These last two factors are subjects of additional discussion in following subsections.

EFFECT OF SEED SIZE

The ability of seeding material to absorb water is primarily a function of its mass. Hence, to a first approximation, whether large or small particles are used does not influence the amount of water that can be absorbed, and the ability of seed material to cause the redistribution of the water content of fog from natural nuclei to seed nuclei is primarily a function of the mass density of the seeds. The reduction of visibility caused by the seed particles themselves is a function of their size and number density. Thus, for a given ability of the seeds to cause the dehydration of the natural fog ("absorptive power" of the artificial nuclei), it seems reasonable to choose a few large seed particles rather than many small ones. From another point of view, one can desiccate natural fog particles more effectively by seeding the same number density of large particles as one might of small particles (because the seed mass is increased). Also of importance is the fact that if fewer larger seed particles are employed, they will grow larger and fall out more quickly, carrying with them more fog water than if small particles were used.

These expectations are verified by the entries in Tables 3 and 4, which suggest that the larger the seed particle used, the greater the improvement in visibility one might expect by seeding. In the case of 80μ seeds, the predicted visibility improvement is remarkable. Although the general trend depicted in these tables seems reasonable, there are compelling reasons to question the value of the predictions with regard to the larger seeds. The model treats the cloud as being homogeneous, with no relative motion between fog particles and environment. The vapor-density field surrounding each particle is assumed unaffected by other particles, and Laplace's equation is assumed valid. At the peak

in visual range predicted for seeding 512 mg/m^3 of 80μ seeds, the seeds have grown to 230μ in diameter, and most have fallen out of the cloud, carrying the fog water with them. Only about 300 seed particles/m^3 remain. The terminal velocity of the remaining particles is high enough to require the use of a ventilation factor in calculating their growth, and it is questionable whether such a small number of falling particles would have other than a local effect on the vapor density. It should also be borne in mind that there is a practical limit to the mass density of seed material that can be economically dispersed, or that, after fallout to the ground, would give a permissible level of pollution. The latter, of course, would be a function of the chemical composition of the seeds.

Figure 16 contains data on the effectiveness of 4 and 5μ seed particles. Equal masses (8 mg/m^3) of seed material were simulated in these experiments; consequently, more than twice as many 4μ as 5μ seeds were required to maintain a constant initial mass density. The concentration of 4μ seeds (120 cm^{-3}) is relatively large, and hence the seed-containing droplets significantly decrease visibility. There are so many 4μ seeds that they do not grow quickly. Consequently they fall out of the cloud slowly, and visibility only slowly improves. It is of interest to note that for the 4μ seeds the water vapor density remains below saturation for a longer period of time and attains lower values than for 5μ seeding. This is a direct consequence of the fact that a greater mass of seed material remains in the 4μ seeded fog as a result of the slower growth and lower terminal velocity of the droplets grown on the large number of seed particles. Seeds much smaller than 4μ are expected to be ineffective.

Figure 17 contains data similar to those of Fig. 16, except that much larger seeds have been simulated. In the illustrated experiments, 32 mg/m^3 of seed material was simulated. Significant clearing is predicted for 20μ seeds, but very little for 40μ seeds [and virtually none for 80μ seeds (not shown)]. In these cases the absence of clearing for large seeds is related to their rapid growth, fall out, and consequent low number density and inability to absorb water rapidly from the cloud. A comparison of Figs. 16 and 17 emphasizes the fact that the proper mass concentration of seeds is size dependent.

in visual range predicted for seeding 512 mg/m^3 of 80μ seeds, the seeds have grown to 230μ in diameter, and most have fallen out of the cloud, carrying the fog water with them. Only about 300 seed particles/m^3 remain. The terminal velocity of the remaining particles is high enough to require the use of a ventilation factor in calculating their growth, and it is questionable whether such a small number of falling particles would have other than a local effect on the vapor density. It should also be borne in mind that there is a practical limit to the mass density of seed material that can be economically dispersed, or that, after fallout to the ground, would give a permissible level of pollution. The latter, of course, would be a function of the chemical composition of the seeds.

Figure 16 contains data on the effectiveness of 4 and 5μ seed particles. Equal masses (8 mg/m^3) of seed material were simulated in these experiments; consequently, more than twice as many 4μ as 5μ seeds were required to maintain a constant initial mass density. The concentration of 4μ seeds (120 cm^{-3}) is relatively large, and hence the seed-containing droplets significantly decrease visibility. There are so many 4μ seeds that they do not grow quickly. Consequently they fall out of the cloud slowly, and visibility only slowly improves. It is of interest to note that for the 4μ seeds the water vapor density remains below saturation for a longer period of time and attains lower values than for 5μ seeding. This is a direct consequence of the fact that a greater mass of seed material remains in the 4μ seeded fog as a result of the slower growth and lower terminal velocity of the droplets grown on the large number of seed particles. Seeds much smaller than 4μ are expected to be ineffective.

Figure 17 contains data similar to those of Fig. 16, except that much larger seeds have been simulated. In the illustrated experiments, 32 mg/m^3 of seed material was simulated. Significant clearing is predicted for 20μ seeds, but very little for 40μ seeds [and virtually none for 80μ seeds (not shown)]. In these cases the absence of clearing for large seeds is related to their rapid growth, fall out, and consequent low number density and inability to absorb water rapidly from the cloud. A comparison of Figs. 16 and 17 emphasizes the fact that the proper mass concentration of seeds is size dependent.

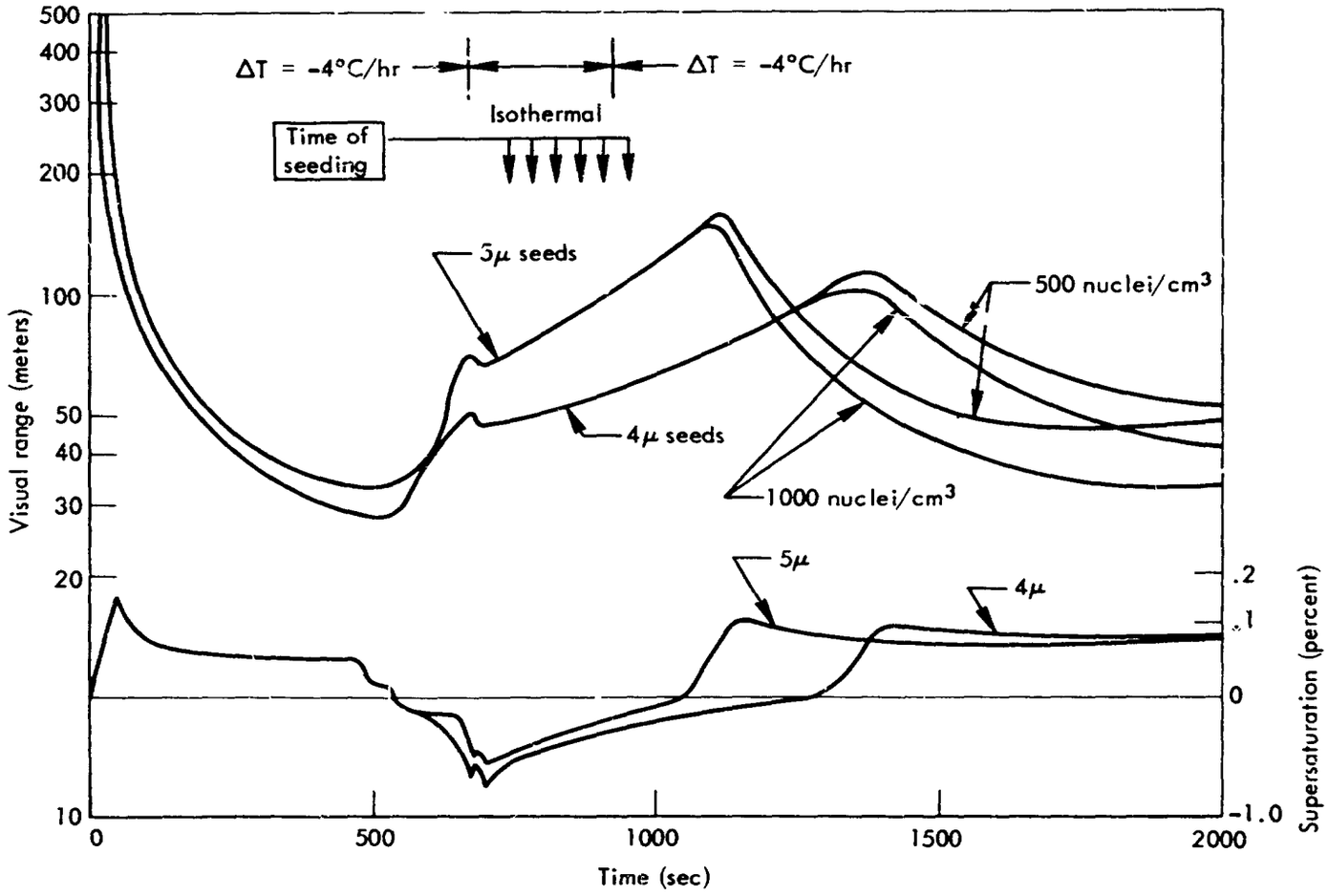

Fig. 16 -- Comparison of predicted change in visual (meteorological) range with time, using original air having various aerosol contents, and using constant seed mass concentrations ($8mg/cm^3$) but different sizes and, consequently, different number concentrations. Aerosol concentration peaked at 0.1μ diameter; cloud 9m thick.

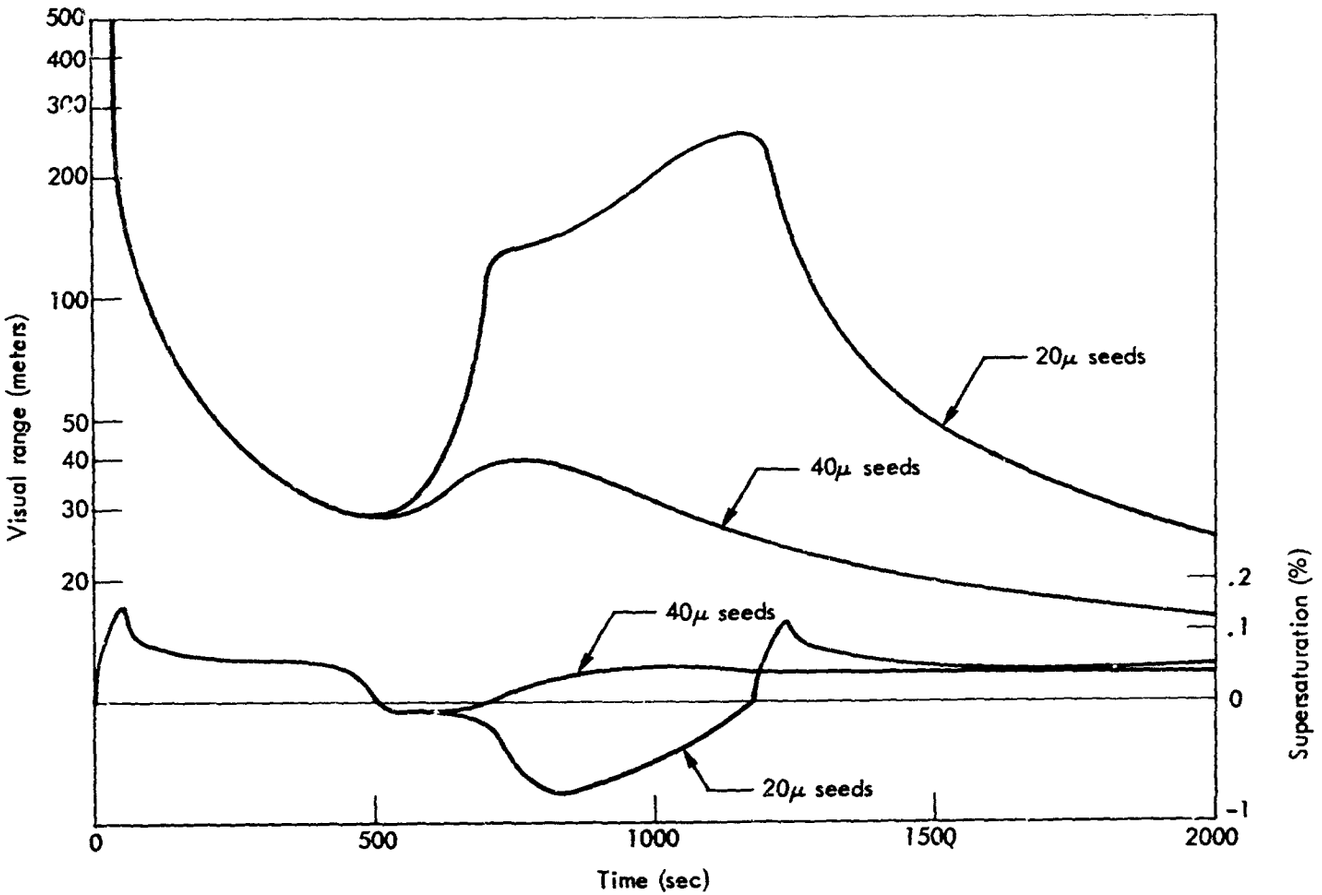

Fig. 17 -- Comparison of predicted change in visual (meteorological) range with time, using constant seed mass concentrations but different sizes and consequently, different number concentration. Original aerosol contained 500 particles/ cm^3 peaked at 0.1μ diameter; cloud 90m thick. Cooling rate, -4°C/hour.

EFFECT OF DIFFERENCES IN FOG THICKNESS

Fog thickness influences the numerical prediction because of its effect on the period of time that a drop or seed particle remains in the fog. Three thicknesses of fog were simulated: 9 m, 90 m, and infinite. The first might be applicable to radiation fogs, but was chosen in order to predict what might occur in the Cornell laboratory chamber under various circumstances; the second was chosen to simulate more common natural-fog situations; and the last, to remove the effects of drop fallout. Fallout was simulated by subtracting from the total number of droplets, for each size, the number of drops present, multiplied by the distance they would fall during the time step, divided by the thickness of the cloud. Thus, in effect, the cloud was assumed homogeneous before each time step. Therefore, even if, for a certain size category, the sum of the fall distance during several time steps exceeded the thickness of the fog, some drops would remain.

If seed particles fall through the fog before their full potential to absorb water is realized they are inefficiently utilized, and a large amount of seed material is required. If, on the other hand, the fog is so thick that seed particles remain until they become, in effect, infinitely dilute before falling out, the seed loses much of its potential as a fog-suppressing agent, and visibility is improved solely as a result of the redistribution of the water content of the fog from many to fewer droplets.

The period of effectiveness of a seed particle is a function of its size and of the water-vapor density of the environment to which it is exposed. The latter factor is a function of the mass of seed material employed and the degree of activity of the fog-producing process. On the basis of Figs. 5, 6, 11, and 12, we conclude that the duration of effectiveness is approximately the period in which the ambient vapor density is below saturation.

Table 4 summarizes the results of several experiments bearing on the effect of fog thickness on seedability. It is apparent that seed particles 5μ in diameter could be used to improve the visibility in a 9-m-thick fog, but would be of little value in a fog 90 m or greater in thickness. The thicker fog requires larger particles and a greater

Table 4

INFLUENCE OF CLOUD DEPTH ON VISIBILITY IMPROVEMENT[a]

Simulated Condition			Visual Range		Time at Max. Visual Range (sec)	Ratio Visual Range (Max/Min)
Cloud Depth (meters)	Seed Parameter: Diameter (microns)	Seed Parameter: Mass (milligrams)	Min. (m)	Max. (m)		
Infinite	5	8	29	47	690	1.6
90	5	8	29	52	680	1.8
9	5	8	29	160	1,110	5.5
90	5	4	29	54	920	1.9
9	5	4	33	92	900	2.8
90	10	16	29	97	1,500	3.3
9	10	16	35	631	931	18.0
90	20	32	29	257	1,150	8.9
9	20	32	35	250	761	7.2
90	40	64	29	373	960	12.8
9	40	64	35	69	721	2.0
90	80	512	29	24,700	1,490	850.0
9	80	512	35	421	741	12.0

[a]All experiments were with 500 natural aerosol particles/cm^3 and a peak concentration at 0.1μ diameter; cooling rate was 4°C/hr.

mass of seeding material per unit volume. Relatively large particles can be used for seeding thin clouds. If particles are larger than "optimum" size, fewer are needed, but there must be a greater mass per unit volume.

A factor not adequately accounted for in the numerical experiment is the time over which a particular volume of fog is exposed to seed particles. Large, rapidly falling particles may fall through a particular volume too quickly for significant amounts of water vapor to diffuse from fog droplets to seed particles. In this case, clearing would be less than predicted, as the experiment assumes homogeneous mixing.

EFFECTS OF VARIATIONS IN RAPIDITY OF DISPERSAL

To approximate the conditions of the Cornell experiment, seed materials were generally introduced in six lots, each separated by 30 simulated seconds. In a few cases all seed material was introduced at once, and in a few others, seeding was extended over longer periods (up to 24 minutes maximum). In general, one batch of seed material lowers the value of the minimum water-vapor density but maintains subsaturation for a shorter time than does multibatch seeding. Results generally indicate that if all seed material is introduced before the time of maximum clearing for single-dose seeding, there is little difference in effectiveness. There is less visibility improvement if seeding continues beyond the time of maximum clearing for a single dose (total mass concentration identical). These results are based on experiments with seeds so small that the drops they form do not fall out rapidly. On the other hand, one may assume that if the seeds are so large that they fall out during continuous seeding, water is continually removed from the fog and thus visibility is continually improved. Small seeds remain within the fog after losing their effectiveness, and tend to contribute to poor visibility; large seeds fall out.

Slow seeding of relatively small seed particles is ineffective because seed particles having a low mass density cannot absorb sufficient fog water to significantly lower the water-vapor density below

saturation, and consequently the evaporation of natural fog droplets is insufficient to cause much visibility improvement. Furthermore, the seeds themselves soon grow large enough to behave like infinitely dilute droplets, and are indistinguishable from natural fog droplets with regard to their ability to absorb water.

Continual seeding with relatively large particles has merit if the large droplets thereby formed fall out of the fog, thus lowering its water content.

A thin fog can be quickly cleared by one application of large seed particles. If an active fog-producing mechanism is present, however, the fog quickly re-establishes itself, and, in general, the larger the seeds the greater the mass concentration needed.

EFFECT OF DIFFERENCES IN NATURAL AEROSOL CONCENTRATION AND SIZE DISTRIBUTION

Natural aerosols in the atmosphere were modeled using input parameters for 27 different sizes of sodium chloride particles (Table 1). Numerical experiments were made using aerosol particle concentrations ranging from 250 to 10,000 particles/cm^3 with constant relative concentration, the mode aerosol diameter being 0.1μ. Results of experiments using 500 and 1000 nuclei/cm^3 and two different seed dosages are shown in Fig. 16. A comparison of results using concentrations of 500, 1000, and 10,000 particles/cm^3 indicates that minimum visual ranges are equal before seeding and that maximum visual range increases with decreasing aerosol content. This suggests that fog formed in a "clean" atmosphere is more susceptible to artificial modification than fog formed in a "dirty" atmosphere. As shown in Table 5, however, the differences are not remarkable, and in a field effort, it is doubtful whether the aerosol content of the air will detectably influence its seedability.

Results with an aerosol concentration of 250 particles/cm^3 reversed this trend. Although a greater maximum visual range was achieved in "seeding" this fog, the minimum visual range was 50 percent greater than in the other three cases, and the overall percentage improvement

Table 5

INFLUENCE OF INITIAL AEROSOL CONCENTRATION ON VISIBILITY IMPROVEMENT[a]

Simulated Condition			Visual Range		Time at Max. Visual Range (sec)	Ratio Visual Range (Max/Min)
	Seed Parameter					
Aerosol Concentration	Diameter (microns)	Mass (milligrams)	Min. (m)	Max. (m)		
250	5	8	45	176	1,140	3.9
500	5	8	29	160	1,110	5.5
1,000	5	8	29	142	1,090	4.9
10,000	5	8	23	75	990	3.2

[a]All experiments were conducted using an aerosol size distribution peaking at a diameter of 0.1μ and a cooling rate of 4°C/hr.

less. The greater minimum visual range resulted from the fact that when the fog is composed of fewer droplets, they grow more rapidly than do droplets when the concentration of aerosols is higher. Greater supersaturations occur in fogs formed in relatively clean air. This is a consequence of the necessity to activate relatively small aerosol particles, and leads to more rapid growth of those droplets that are formed. Since, for a given fog water content, the visual range is proportional to the mean diameter of the droplets, the natural fog formed in clean air is more transparent than that formed in dirty air. This effect may be somewhat overstated in the numerical prediction, which reflects a discontinuous size distribution of aerosols.

The use of an aerosol concentration of $10,000/cm^3$ does not result in an absurdly large number of fog droplets. At the time of minimum visual range, there are 200 droplets 10μ or larger in diameter and 1000 larger than 5μ. If an aerosol concentration of $1000/cm^3$ is used, there are 400 droplets 10μ or larger in diameter and 500 larger than 5μ.

Numerical experiments were made using two different aerosol size distributions having mode diameters of 0.1 and 0.35μ, respectively (Table 6). The former distribution was intended to approximate a continental air mass. Everything else being the same, fog formed in the air mass having the smaller-mode-size aerosol was found to be the more susceptible to seeding. The difference occurred predominantly in the maximum visual range achieved after seeding, rather than in the minimum visual range before seeding.

EFFECT OF MONODISPERSED SEED PARTICLES IN CONTRAST TO THAT OF POLYDISPERSED SEED PARTICLES

To examine the influence of seed size, seeding was simulated in most of the numerical experiments by means of monodispersed seed particles. To simulate the Cornell experiments, several experiments were made using a polydispersed seed. A comparison of the results achieved (cf. Figs. 11 and 16) indicates that whereas the maximum visibility improvement may be similar in both cases, the period of time in which

Table 6

INFLUENCE OF INITIAL AEROSOL SIZE DISTRIBUTION ON VISIBILITY IMPROVEMENT[a]

Simulated Condition			Visual Range		Time at Max. Visual Range (sec)	Ratio Visual Range (Max/Min)
	Seed Parameter					
Aerosol Spectrum[b]	Diameter (microns)	Mass (milligrams)	Min. (m)	Max. (m)		
.35	5	8	32	116	1,050	3.6
.10	5	8	29	160	1,110	5.5
.35	5	4	32	88	860	2.7
.10	5	4	33	97	900	2.9
.35	5	2	32	42	800	1.3
.10	5	2	33	44	800	1.3
.35	4	8	32	86	1,330	2.7
.10	4	8	34	116	1,380	3.4

[a]All experiments were with 500 natural aerosol particles/cm^3 and a cooling rate of 4°C/hr.

[b]Number refers to size (in microns) of modal value of aerosol in spectrum; see Table 1 for comparison among the spectra used.

visibility remains near the maximum is considerably shorter for monodispersed seeds than for polydispersed seeds. This suggests that monodispersed seed particles are not ideal, and a distribution of seed sizes appears more desirable.

EFFECT OF DROPLET FALLOUT

The initial improvement in visibility in a seeded fog results from the redistribution of the water content from the many natural droplets toward the artificially produced droplets. Because of their large nuclei, these seed-produced droplets grow relatively large, and typically attain appreciable terminal velocities relative to droplets containing natural nuclei. Visibility is improved by the fallout of the seed particles, which remove liquid water from the fog. If the fog-forming process stops, the visibility improvement should be more or less permanent (neglecting turbulent mixing with untreated, foggy air). In our experiments, the fog-forming process continued after seeding was simulated. As a result, after seed-containing droplets had substantially fallen out, condensation once more occurred on the natural fog droplets, and visibility again decreased. During the period in which seed particles are effective, the water-vapor density falls below saturation, and the subsequent rise of vapor density above saturation signals the end of the effectiveness of the seed particles and serves as a harbinger of lower visibility. This sequence of events is graphically shown on many of the accompanying figures (e.g., Figs. 11 and 15).

V. CONCLUSIONS

The numerical model of fog microphysics used in this study supports the following generalizations:

1. Visibility within fogs can in principle be usefully improved by seeding with condensation nuclei.

2. The greater the mass density of seed particles, the greater will be their effectiveness in evaporating natural fog droplets and reducing their ability to restrict visibility.

3. The greater the number density of seed particles, the greater will be the number density of fog particles formed upon seed material, and consequently the greater will be the reduction in visibility caused by the seed particles themselves.

4. When one attempts to maximize the transparency of fog, the visibility restriction due to both natural and artificial fog particles must be considered. Large quantities of seed material may reduce the undesirable effects of natural fog particles, but may constitute an even greater source of visibility restriction.

5. For a given mass density of seeds, the larger the seed particles, the more quickly clearing occurs. The use of larger particles, however, does not necessarily produce greater visibility.

6. A properly chosen monodispersed seeding material will produce maximum clearing, but the visibility remains high for a shorter period of time than that achieved by use of a properly chosen polydispersed material. The latter seems preferable to allow variation in translation of a cleared volume to the desired location and to allow useful time to accomplish the mission whose undertaking instigated the seeding.

7. The thickness of the fog to be cleared is a factor to be considered in choosing seed material, particularly if the smallest possible seeds are desired. During their fall through a fog, seed particles must be able to absorb water at the expense of natural particles throughout the period of fall. In a thick fog, in which the time of fall from seed level to the base of the fog is longer than in a thin fog, seed particles must thus be larger.

8. The microphysical properties of the natural fog, drop size distribution, drop concentration, and aerosol concentration have secondary, minor influences on the effectiveness of seeding a fog.

The present numerical work should be useful as a guide for field experimentation in warm-fog suppression. Since, however, we have attempted to model neither the real atmosphere nor plausible dispersal characteristics of seeding systems, some interpretation is necessary to translate the numerical work to field applications. In particular, we have made no attempt to account for the ambient horizontal wind or the mixing of seeded and unseeded portions of the fog. Although such mixing will initially help to disperse the seed materials properly, later mixing will destroy the clearing achieved. It seems probable that the greater the mixing within the fog and the greater the ambient wind, the faster one would want to achieve clearing. This suggests the use of large seed particles and high mass concentration.

REFERENCES

Fletcher, N. H., 1962: THE PHYSICS OF RAINCLOUDS. Cambridge University Press. 386 pp.

Gunn, R. and G. D. Kinzer, 1949: The terminal velocity of fall for water droplets in air. J. Meteor, 6, 243-248.

Juisto J. E., R. J. Pilié and W. C. Kocmond, 1968: Fog modification with giant hygroscopic nuclei. J. Appl. Meteor., 7, 860-869.

Koenig, L. R., 1968: NUMERICAL MODELING OF CONDENSATION. RM-5553-NSF. The RAND Corporation, Santa Monica, California. 43 pp.

List, R. J., 1966: SMITHSONIAN METEOROLOGICAL TABLES. The Smithsonian Institution, Washington, D. C. 527 pp.

Middleton, W. E. K., 1952: VISION THROUGH THE ATMOSPHERE. University of Toronto Press. 250 pp.

Pilié, R. J., W. C. Kocmond and J. E. Juisto, 1967: Warm fog suppression in large scale laboratory experiments. Science, 157, 1319-1320.

Wieland, W., 1956: Die Wasserdamf kondensation an naturlichem Aerosol bei geringen Ubersattigungen. Eidg. Tech Hochsch. Zurich, Promotionsarbeit No. 2577. (Cited by Fletcher, N. H., 1962: THE PHYSICS OF RAINCLOUDS. Cambridge University Press. 386 pp.)

DOCUMENT CONTROL DATA

1 ORIGINATING ACTIVITY	2a. REPORT SECURITY CLASSIFICATION
THE RAND CORPORATION	UNCLASSIFIED
	2b. GROUP

3. REPORT TITLE

NUMERICAL EXPERIMENTS PERTAINING TO WARM-FOG SUPPRESSION

4. AUTHOR(S) (Last name, first name, initial)

Koenig, L. R.

5. REPORT DATE	6a. TOTAL No. OF PAGES	6b. No. OF REFS.
October 1969	60	8

7. CONTRACT OR GRANT No.	8. ORIGINATOR'S REPORT No.
F44620-67-C-0045	RM-6159-PR

9a AVAILABILITY/LIMITATION NOTICES	9b. SPONSORING AGENCY
DDC-1	United States Air Force Project RAND

10. ABSTRACT

An examination of the problems involved in applying seeding techniques for the improvement of visibility in natural warm fogs. This Memorandum presents a quantitative assessment of the prospects of modifying warm fogs, i.e., fogs composed of droplets warmer than 0 deg C, by seeding them with condensation nuclei. In the experiments performed, initial conditions consist of a homogeneous volume of air of specified height and aerosol content. An external cooling rate and seed dosage are specified. The effects of various combinations of cloud height, seed properties (such as size, mass density, and rate of injection) and the metamorphosis of the fog-droplet population are examined. The cloud-forming process is allowed to continue after seeding has been accomplished, and tentative conclusions are drawn regarding the ranges of seed dosages that might result in successful efforts to suppress warm fog. A discussion of the basis of the calculations of the meteorological range is included.

11. KEY WORDS

Weather
Meteorology
Clouds
Numerican methods and processes